energies

Article

Thermodynamic Analysis and Improvement Potential of Helium Closed Cycle Gas Turbine Power Plant at Four Loads

Vedran Mrzljak [1,*], Igor Poljak [2], Maro Jelić [3] and Jasna Prpić-Oršić [1]

[1] Faculty of Engineering, University of Rijeka, Vukovarska 58, 51000 Rijeka, Croatia
[2] Department of Maritime Sciences, University of Zadar, Mihovila Pavlinovića 1, 23000 Zadar, Croatia
[3] Maritime Department, University of Dubrovnik, Ćira Carića 4, 20000 Dubrovnik, Croatia
* Correspondence: vedran.mrzljak@riteh.hr; Tel.: +385-51-651-551

Abstract: This paper presents thermodynamic and improvement potential analyses of a helium closed-cycle gas turbine power plant (Oberhausen II) and dominant plant components at four loads. DESIGN LOAD represents optimal operating conditions that cannot be obtained in exploitation but can be used as a guideline for further improvements. In real plant exploitation, the highest plant efficiency is obtained at NOMINAL LOAD (31.27%). Considering all observed components, the regenerator (helium-helium heat exchanger) is the most sensitive to the ambient temperature change. An exact comparison shows that the efficiency decrease of an open-cycle gas turbine power plant during load decrease is approximately two and a half or more times higher in comparison to a closed-cycle gas turbine power plant. Plant improvement potential related to all turbomachines leads to the conclusion that further improvement of the most efficient turbomachine (High Pressure Turbine—HPT) will increase whole plant efficiency more than improvement of any other turbomachine. An increase in the HPT isentropic efficiency of 1% will result in an average increase in whole plant efficiency of more than 0.35% at all loads during plant exploitation. In the final part of this research, it is investigated whether the additional heater involvement in the plant operation results in a satisfactory increase in power plant efficiency. It is concluded that in real exploitation conditions (by assuming a reasonable helium pressure drop of 5% in the additional heater), an additional heating process cannot be an improvement possibility for the Oberhausen II power plant.

Keywords: thermodynamic analysis; Oberhausen II; closed cycle gas turbine power plant; helium; various plant loads; improvement potential

check for updates

Citation: Mrzljak, V.; Poljak, I.; Jelić, M.; Prpić-Oršić, J. Thermodynamic Analysis and Improvement Potential of Helium Closed Cycle Gas Turbine Power Plant at Four Loads. *Energies* **2023**, *16*, 5589. https://doi.org/10.3390/en16155589

Academic Editor: Antonio Calvo Hernández

Received: 26 June 2023
Revised: 17 July 2023
Accepted: 21 July 2023
Published: 25 July 2023

1. Introduction

Gas turbine power plants are nowadays widely used in various practical applications. Its dominant usage is evident in mechanical power production, where they operate as independent mechanical power producers [1,2] or as a part of various complex systems for mechanical power and/or heat production [3–5]. The high combustion gas temperature at the gas turbine power plant outlet allows heat utilization and efficiency increases for the entire system in which they operate [6,7]. In marine propulsion, gas turbine power plants can be found inside many complex systems [8,9], but due to their high costs, they are rarely found as independent propulsion elements [10]. Gas turbine power plants are also the base elements of aircraft jet engines, regardless of jet engine type (turbojet, turbofan, turboshaft, or turboprop) [11–16]. Therefore, the wide usage of gas turbine power plants is obvious in many practical engineering applications.

Open-cycle and closed-cycle are the two main types of gas turbine power plants. Open-cycle gas turbine power plants use air from the atmosphere and release combustion gases into the atmosphere; therefore, their connection to the environment is essential for operation [17]. The majority of gas turbine power plants mentioned above in various applications are open-cycle.

In relation to open-cycle gas turbine power plants, closed-cycle gas turbine power plants did not require any connection to the environment. Inside closed-cycle gas turbine power plants, the same gas (operating fluid) is always circulated, which is compressed in a turbocompressor, heated in the main heater, expanded in the gas turbine, and finally cooled before another compression [18]. The same procedure is constantly repeated during closed-cycle gas turbine power plant operations. Operating fluids used in closed-cycle gas turbine power plants are helium, neon, argon, CO_2, nitrogen, or other similar gases that are inert to metal parts and have satisfactory thermophysical properties. Selected operating fluid characteristics substantially widen the list of metals suitable for making turbomachinery blades and other plant components [19]. Closed-cycle gas turbine power plants can also be used in nuclear power systems where a nuclear reactor is used as the main heater [20,21].

There are many advantages to closed-cycle gas turbine power plants in comparison to open-cycle gas turbine power plants, but at the same time, there are also several disadvantages. The main disadvantage is that the main heat exchangers (coolers and heaters) in closed-cycle gas turbine power plants have huge dimensions (comparable to steam generators and condensers in steam power plants) due to the large surfaces required for efficient heat transfer [22]. Also, the majority of the mentioned operating fluids in closed-cycle gas turbine power plants have a high fluidity (which results in sealing problems), are expensive, and are not always achievable in the market [23].

Closed-cycle gas turbine power plants are dominantly used for mechanical power production, as confirmed by Olumayegun et al. in a review [24]. The best characteristics of all operating fluids used in closed-cycle gas turbine power plants show helium, so McDonald [25] performed a review of helium turbomachinery operating experience from gas turbine power plants and test facilities. Kunniyoor et al. presented many designs and improvements for closed-cycle gas turbine power plants at various operating conditions [26]. Al-attab and Zainal [27] concluded that the main heater in a closed-cycle gas turbine power plant is the key element whose operation has the most notable influence on the plant's operation and efficiency.

Closed-cycle gas turbine power plants found application also in marine systems. Hou et al. [28] presented an analysis of supercritical CO_2 recompression and the regenerative cycle used in waste heat recovery in marine gas turbine power plants. Similar research related to supercritical CO_2 closed-cycle gas turbine power plants used in marine waste heat recovery systems can be found in [29,30]. It can be concluded that in marine applications, closed-cycle gas turbine power plants are dominantly used for additional mechanical power production from waste heat. A favorable marine closed-cycle gas turbine process is a supercritical CO_2 process.

Recently, closed-cycle gas turbine power plants operated as a part of various complex systems for mechanical power production or as a part of various Combined Heat and Power (CHP) systems [31–34]. Also, researchers nowadays investigate the usage of various mixtures (instead of only one gas) as operating fluids in closed-cycle gas turbine power plants [35]. Finally, from the literature review, it can be concluded that closed-cycle gas turbine power plants are important elements in the research community.

In the literature, there are several studies and reviews that, among others, deal with Oberhausen II (a helium closed cycle gas turbine power plant), its characteristics, specifications, and operating parameters [19,25,36–39]. This paper will fill the literature gap because plant operating parameters at several loads will be arranged in one place (at the moment they can be partially composed from various literature sources, while the details require additional calculations). Isentropic, energy, and exergy analyses of this power plant and its dominant components have not been performed so far at any plant load. It is unknown which component is most influenced by the ambient temperature change. In the literature, there is no exact comparison between closed-cycle and open-cycle gas turbine power plants related to the plant efficiency decrease intensity at partial loads. Moreover, it is investigated the influence of each observed component isentropic (or energy) efficiency increase on the whole plant efficiency. In that way, components are detected whose improvement will be the most influential to the whole plant process. Finally, for the Oberhausen II power plant, improvement potential is investigated by involving additional heaters in the plant's operation.

2. Description and Operating Characteristics of the Oberhausen II Power Plant

2.1. Power Plant Background

The Oberhausen II helium closed cycle gas turbine power plant was designed and built with the aim of satisfying two major functions:

- To operate as a commercial power plant that will deliver electrical power and heat to the city of Oberhausen,
- To provide data applicable for the further nuclear gas turbine project, especially considering the dynamic behavior of the entire power plant. Also, it was important to obtain long-term operation experience for the major plant components in the helium environment (especially turbomachines).

In the further planned nuclear gas turbine project, the design values of the helium temperature and pressure at the turbine inlet were 850 °C and 60 bar, respectively. So high a helium temperature cannot be achieved in the Oberhausen II plant, and a helium temperature at the turbine inlet of 750 °C was selected due to tube material stress considerations in the external coke oven burner. At design load, a maximum system pressure of only 28.5 bar was selected so that the helium volumetric flow corresponded to a much larger helium turbomachine. This would result in representative stress loadings and allow a reasonable extrapolation to the larger machine size (of approximately 300 MW) planned for the nuclear helium power plant.

2.2. Base Part of the Oberhausen II Power Plant

The general scheme of the Oberhausen II power plant is presented in Figure 1. As can be seen from Figure 1, a power plant is composed of two parts: the base and the auxiliary part.

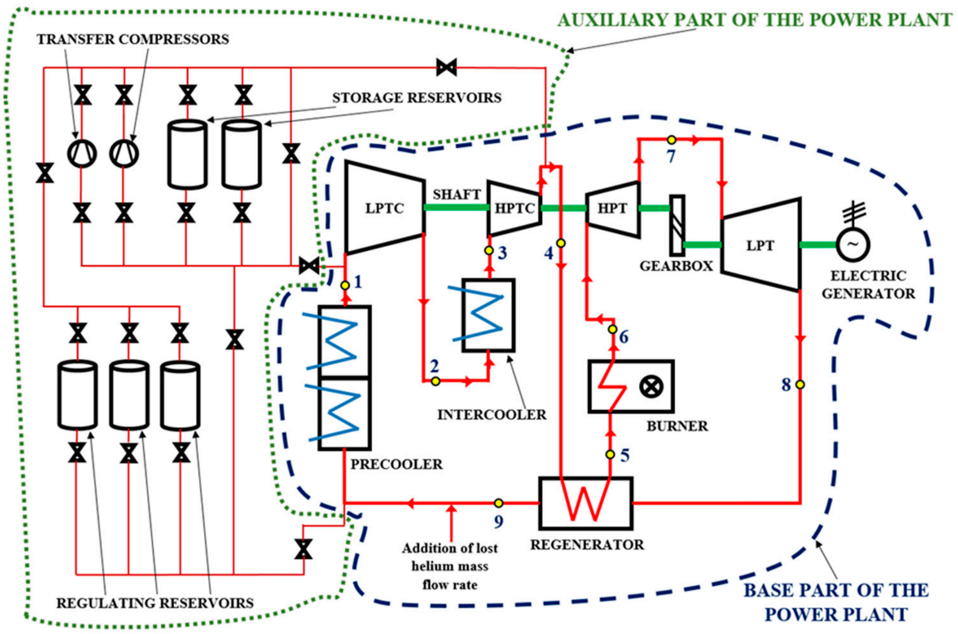

Figure 1. General scheme of the Oberhausen II (helium closed-cycle gas turbine power plant) along with operating points required for the thermodynamic analysis.

The base part of the Oberhausen II power plant consists of four turbomachines: a low-pressure turbocompressor (LPTC), a high-pressure turbocompressor (HPTC), a high-pressure turbine (HPT), and a low-pressure turbine (LPT). Both turbocompressors are axial types; LPTC has 10 stages, while HPTC has 15 stages. The main function of an axial, 7-stage HPT is to produce sufficient mechanical power for both turbocompressor drives, so the HPT and turbocompressors are connected to the same shaft, whose rotational speed is 5500 rpm. Any mechanical power surplus produced in HPT is delivered to the electric generator through the gearbox. LPT is an axial, 11-stage turbine mounted on an independent shaft, and its rotational speed is 3000 rpm. The entire mechanical power produced by the LPT is used for the electric generator drive. At both turbocompressors and LPT, helium leakage occurs through inlet and outlet gland seals, while at HPT, a certain helium mass flow rate is added for sealing and blade cooling purposes. Mentioned helium leakages and additions are incorporated in the presented data at each plant load. The lost helium mass flow rate in turbomachines is added from the auxiliary part of the plant to the main helium flow stream after the regenerator (Figure 1). Finally, it should be stated that each turbomachine is placed in a spherical housing, which notably reduces helium leakage. More details related to each turbomachine can be found in [25,38]. The regenerator is a counter-flow helium-helium heat exchanger where colder helium is preheated (before its entrance to the burner) by using higher-temperature helium, which exits from LPT. The high-pressure (and low-temperature) regenerator part is composed of more than 17,000 horizontal pipes. The precooler (main cooler) is a cross-flow heat exchanger where the helium is cooled to the desired temperature at the LPTC inlet by using cooling water. The precooler is divided into two parts: in the first part (the helium entrance from the regenerator), the cooling water temperature at the precooler outlet is around 120 °C, while in the second part (before LPTC), the cooling water temperature at the precooler outlet is around 40 °C. The cooling water outlet from the first precooler part is used for urban heating purposes, so the observed power plant actually operates as a CHP plant. The intercooler is similar to the second precooler part (helium after compression in LPTC is cooled by using cooling water, whose outlet temperature is around 40 °C). The last component of the base power plant part is the burner (main heater), which uses coke oven gas. In the burner, heat from combustion gases is transferred to helium, which, at the burner outlet, has the highest temperature in the plant (around 750 °C). More details related to the Oberhausen II heat exchangers can be found in the literature [38,39].

2.3. Auxiliary Part of the Oberhausen II Power Plant

The auxiliary part of the power plant is actually the regulation part used for helium mass flow rate delivery to the base plant part or its extraction from the base plant part. In closed-cycle gas turbine power plants, mechanical power is produced by changing the fluid pressure (and consequently the fluid mass flow rate).

The daily fluctuations in heat and power demand are adjusted by using a multi-compartment storage system, which consists of three regulating reservoirs. This system is designed to operate without using transfer compressors. If the helium pressure in the base part of the process has to be reduced, a certain quantity of helium flows from the tapping point downstream of the HPTC into the regulating reservoirs. The regulating reservoirs are filled one after another until the desired equilibrium pressure is obtained. If the helium pressure in the base part of the process has to be raised again, stored helium is allowed to leave the regulating reservoirs and re-enter the base part of the plant before the precooler. Each regulating reservoir has a volume of 120 m^3. It should be highlighted that the number and volume of each regulating reservoir are the results of the optimization calculation. Regulating reservoirs allows a power change rate of approximately 60% per hour.

Two storage reservoirs (each storage reservoir also has a volume of 120 m^3) are used for the long-term storage of the helium when the plant is operating at partial loads for a long period of time. The operation of the transfer compressors is required only for the storage reservoirs' filling [37].

Due to the complete lack of exact data related to the auxiliary part of the Oberhausen II power plant, this paper will analyze only the base plant part. The mechanical power used by the transfer compressors can be neglected in the calculations because they operate for a very short period of time and are not in use during daily helium fluctuations.

2.4. Design Load and Data Availability

In the literature, there are many data points related to the Oberhausen II power plant [19,25,36–39]. However, most of the presented data is related to the DESIGN LOAD. Most of the data used in this analysis is found in [39]. However, many operating parameters at various loads (especially low loads) are not known and are obtained mathematically using various realistic assumptions derived from the literature or experience. Oberhausen II general data at the DESIGN LOAD are presented in Table 1.

Table 1. Oberhausen II general data at the DESIGN LOAD [25,38,39].

Shaft Power Capacity	52.3 MW
Overall pressure ratio	2.7
Helium mass flow rate at the HPT inlet	84.4 kg/s
HPT efficiency	88.3%
LPT efficiency	90.0%
HPTC efficiency	85.5%
LPTC efficiency	87.0%
HPT/HPTC/LPTC inlet temperatures	750 °C/25 °C/25 °C
LPT outlet temperature	460 °C
System pressure loss	10.2%
Plant electric efficiency	~36%

The limited available data related to the Oberhausen II power plant, especially at various plant loads, resulted in some necessary simplifications.

Thermodynamic analysis performed in this paper involves isentropic and exergy analyses of each turbomachine (LPTC, HPTC, HPT, and LPT), as well as energy and exergy analyses of the regenerator and whole plant. For the cooling water in both precooler parts as well as in the intercooler, mass flow rates and exact inlet/outlet pressures and temperatures are not known at any observed plant load. The pressure and temperature of the helium between the two precooler parts are also unknown. For burners, there are unknown combustion gas operating parameters, exact coke-oven gas composition, and other elements required for performing complete burner energy and exergy analyses at any plant load.

Due to the mentioned lack of data, for the precooler and intercooler, cumulative heat can be calculated from helium to cooling water, while for the burner, heat can be calculated from combustion gases to helium at each plant load. Heat transferred from combustion gases to helium in the burner at each plant load is one of the essential parameters for the investigation of improvement possibilities. Moreover, in the thermodynamic analysis performed at each of the four observed plant loads, Oberhausen II is considered a plant that produces electricity only (urban heating is neglected due to unknown cooling water exact data from the first precooler part).

In the available literature, which also deals with the Oberhausen II power plant, the same simplifications are adopted [38,39].

3. Equations for the Thermodynamic Analysis

In this paper, isentropic, energy, and exergy analyses will be used for the performance research of each observed plant component and for the whole plant.

The isentropic analysis will be used for the performance observation of each turbomachine inside the Oberhausen II power plant (LPTC, HPTC, HPT, and LPT). The isentropic analysis is based on a comparison between ideal (isentropic) and real (polytropic) expansion processes in any turbine or compression processes in any turbocompressor [40]. Data for the real (polytropic) compression or expansion processes are obtained from the measurements during the plant operation, while the data for ideal (isentropic) compression or expansion are numerically obtained for the process without any losses.

Energy analysis will be used for the performance analysis of the regenerator and the whole power plant. The results of this analysis will be used as a baseline in the investigation of whole plant improvement possibilities. Energy analysis is based on the first law of thermodynamics and does not consider the conditions of the ambient environment in which the analyzed system or component operates [41].

In contrast to energy analysis, exergy analysis is based on the second law of thermodynamics and considers ambient conditions [42]. Exergy analysis will be used for the performance evaluation of all components observed in this power plant as well as for the whole plant. Moreover, exergy analysis will be used in the investigation of the ambient temperature change's influence on each observed plant component's efficiency.

In the recent literature, it can be found that due to some limitations related to isentropic and energy analyses [43], exergy analysis is more widely used in the observation of various energy systems and components [44–46]. Also, exergy analysis can be a baseline for further, more complex analyses [47–51].

3.1. General Equations and Balances

The isentropic analysis used for the turbomachine's operation observation is based on the comparison of real (polytropic) and ideal (isentropic) mechanical power used or produced by the turbomachine. The real (polytropic) mechanical power calculation is based on the fluid operating parameters measured in the power plant (at each turbomachine inlet and outlet). For mechanical power producers and consumers, real (polytropic) mechanical power can be calculated as:

$$\mathrm{P_{PT,producer}} = \dot{\mathrm{m}}\cdot(\mathrm{h_{in}} - \mathrm{h_{out}}), \tag{1}$$

$$\mathrm{P_{PT,consumer}} = \dot{\mathrm{m}}\cdot(\mathrm{h_{out}} - \mathrm{h_{in}}). \tag{2}$$

The ideal (isentropic) process is the process between the same pressures; it uses the same mass flow rates as the real (polytropic) process, but this process always assumes the same specific entropy during compression or expansion. Produced and consumed mechanical power in the ideal (isentropic) process can be calculated as:

$$\mathrm{P_{IS,producer}} = \dot{\mathrm{m}}\cdot(\mathrm{h_{in}} - \mathrm{h_{out,IS}}), \tag{3}$$

$$\mathrm{P_{IS,consumer}} = \dot{\mathrm{m}}\cdot(\mathrm{h_{out,IS}} - \mathrm{h_{in}}). \tag{4}$$

For mechanical power producers, isentropic loss is the difference between ideal and real mechanical power, while isentropic efficiency is the ratio between real and ideal mechanical power (for any mechanical power producer, ideal mechanical power is higher than the real one). For mechanical power consumers, isentropic loss is the difference between real and ideal mechanical power, while isentropic efficiency is the ratio between ideal and real mechanical power (for any mechanical power consumer, ideal mechanical power is lower than the real one).

Energy analysis is used for the performance analysis of the regenerator and the whole power plant. The main energy balance equation for any component in a steady state, with negligible potential and kinetic energy changes, is [52,53]:

$$\dot{\mathrm{Q}} - \mathrm{P} = \sum \dot{\mathrm{m}}_{\mathrm{out}}\cdot\mathrm{h_{out}} - \sum \dot{\mathrm{m}}_{\mathrm{in}}\cdot\mathrm{h_{in}}. \tag{5}$$

For any heat exchanger, the general energy efficiency equation is [54]:

$$\eta_{\mathrm{en,HE}} = \frac{\text{cumulative energy output}}{\text{cumulative energy input}}, \tag{6}$$

While for the whole power plant, energy efficiency can be calculated as a ratio of real useful mechanical power produced in the plant and cumulative heat transferred from fuel to operating fluid:

$$\eta_{en,WP} = \frac{P_{PT,USEFUL}}{\dot{Q}_{FUEL}}. \tag{7}$$

Exergy analysis is used for the performance evaluation of the whole plant and each observed plant component. The main exergy balance equation for any component in steady state, with negligible potential and kinetic energy changes, is [53,55]:

$$\dot{X}_{heat} - P = \sum \dot{m}_{out} \cdot \varepsilon_{out} - \sum \dot{m}_{in} \cdot \varepsilon_{in} + \dot{E}x_{D}. \tag{8}$$

The specific exergy (ε) of any fluid stream can be calculated as [56,57]:

$$\varepsilon = (h - h_0) - T_0 \cdot (s - s_0), \tag{9}$$

While exergy heat transfer ($\dot{X}_{heat}$) at the temperature T can be calculated, according to [53,56], by an equation:

$$\dot{X}_{heat} = \sum \left(1 - \frac{T_0}{T}\right) \cdot \dot{Q}. \tag{10}$$

The exergy efficiency of any mechanical power producer and consumer is [58]:

$$\eta_{ex,producer} = \frac{P_{PT,producer}}{\sum \dot{m}_{in} \cdot \varepsilon_{in} - \sum \dot{m}_{out} \cdot \varepsilon_{out}}, \tag{11}$$

$$\eta_{ex,consumer} = \frac{\sum \dot{m}_{out} \cdot \varepsilon_{out} - \sum \dot{m}_{in} \cdot \varepsilon_{in}}{P_{PT,consumer}}. \tag{12}$$

General equation for the exergy efficiency calculation of any heat exchanger is [56]:

$$\eta_{ex,HE} = \frac{\text{cumulative exergy output}}{\text{cumulative exergy input}}. \tag{13}$$

The whole power plant's exergy efficiency can be calculated by an equation [52]:

$$\eta_{ex,WP} = \frac{P_{PT,USEFUL}}{\dot{Q}_{FUEL} \cdot EC}, \tag{14}$$

where EC is an exergy coefficient based on the fuel type used in the plant. The mass flow rate balance of any component in each of the observed analyses, which includes all fluid leakages and additions, is [53]:

$$\sum \dot{m}_{in} = \sum \dot{m}_{out}. \tag{15}$$

3.2. Equations for the Isentropic, Energy and Exergy Analyses of Oberhausen II Power Plant and Its Observed Components

For each component and whole power plant, isentropic, energy, and exergy analysis equations are defined according to recommendations from the literature [59–61]. All equations remain identical at any observed power plant load. Markings used in the equations and figures throughout this subsection are related to the operating points from Figure 1.

The isentropic analysis of each turbocompressor (LPTC and HPTC) and each turbine (HPT and LPT) is based on the comparison of real (polytropic) and ideal (isentropic) mechanical power (used by the turbocompressors or produced by the turbines). Specific enthalpy-specific entropy (h-s) diagrams of both ideal and real compression and expansion processes for each turbocompressor and turbine are presented in Figure 2 (operating points of the real processes are marked in accordance with Figure 1).

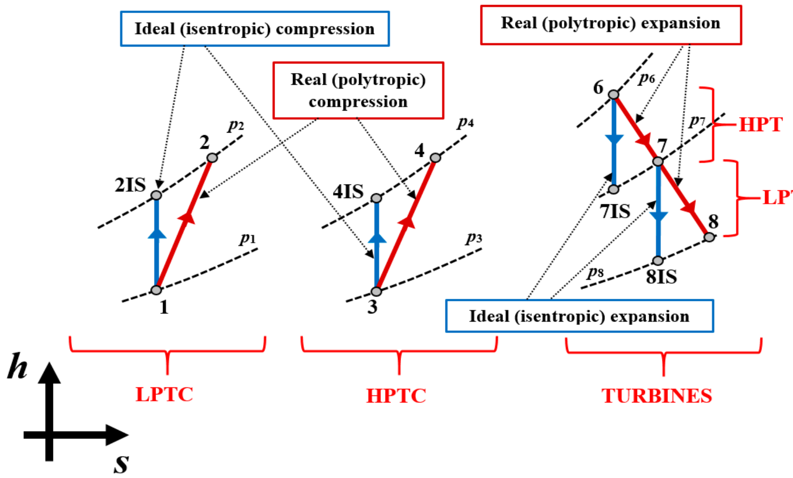

Figure 2. Specific enthalpy—specific entropy (h-s) diagrams for the isentropic analysis of both turbocompressors and turbines.

It should be highlighted that in both analyses related to the turbomachines (isentropic and exergy), relevant helium mass flow rates are inlet mass flow rates to each turbomachine. This simplification must be adopted because LPTC, HPTC, and LPT have helium leakages through both front and rear gland seals, while HPT, which operates with the highest helium pressures and temperatures, has helium additions for sealing and blade cooling purposes. The exact operating parameters of all the mentioned helium leakages and additions are unknown at any plant load, so they must be neglected. However, all leaked or added helium mass flow rates are incorporated in the outlet mass flow rate from each turbomachine (according to the presented data at each load, Appendix A). Standard calculations cannot be applied because they will result in unrealistic results. For example, in the HPT exergy analysis, if the presented outlet mass flow rate is considered (operating point 7, Appendix A), then HPT exergy efficiency will be higher than 100% at each plant load.

Table 2 presents equations for used (turbocompressors), produced (turbines), and useful ideal and real mechanical power. In the Oberhausen II power plant, useful mechanical power is the difference between the cumulative mechanical power produced by both turbines and the cumulative mechanical power used by both turbocompressors. Real (polytropic) useful mechanical power is actually produced in the power plant and used for the electric generator drive. Ideal (isentropic) useful mechanical power is the highest possible mechanical power (at each plant load) that can be used for the electric generator drive in an ideal case (when all the losses in each turbomachine are neglected). Markings in the equations presented in Table 2 are related to operating points from Figures 1 and 2.

Table 2. Equations for the calculation of ideal and real mechanical power (used by turbocompressors, produced by turbines, and useful mechanical power).

	Ideal (Isentropic) Mechanical Power	Equation	Real (Polytropic) Mechanical Power	Equation
LPTC	$P_{IS,LPTC} = \dot{m}_1 \cdot (h_{2IS} - h_1)$	(16)	$P_{PT,LPTC} = \dot{m}_1 \cdot (h_2 - h_1)$	(17)
HPTC	$P_{IS,HPTC} = \dot{m}_3 \cdot (h_{4IS} - h_3)$	(18)	$P_{PT,HPTC} = \dot{m}_3 \cdot (h_4 - h_3)$	(19)
HPT	$P_{IS,HPT} = \dot{m}_6 \cdot (h_6 - h_{7IS})$	(20)	$P_{PT,HPT} = \dot{m}_6 \cdot (h_6 - h_7)$	(21)
LPT	$P_{IS,LPT} = \dot{m}_7 \cdot (h_7 - h_{8IS})$	(22)	$P_{PT,LPT} = \dot{m}_7 \cdot (h_7 - h_8)$	(23)
USEFUL	$P_{IS,USEFUL} = P_{IS,HPT} + P_{IS,LPT} - P_{IS,HPTC} - P_{IS,LPTC}$	(24)	$P_{PT,USEFUL} = P_{PT,HPT} + P_{PT,LPT} - P_{PT,HPTC} - P_{PT,LPTC}$	(25)

HPT and LPT isentropic losses are the difference between ideal and real mechanical power, while the isentropic efficiency of each turbine is the ratio of real and ideal mechanical power. The isentropic loss of LPTC and HPTC is the difference between real and ideal mechanical power, while the isentropic efficiency of each turbocompressor is the ratio of ideal and real mechanical power.

Although the Oberhausen II power plant burner and both coolers (precooler and intercooler) cannot be analyzed in detail due to a lack of complete data, for those components, heat is transferred to helium by fuel (in the burner) and heat is transferred from helium to cooling water (in both coolers). Especially important is the heat transferred to helium by fuel in the burner because its reduction will notably increase whole plant efficiency (Equations (7) and (14)). Moreover, in the research related to plant improvement potential, the burner does not have to be the only component that uses fuel, so in Equations (7) and (14) the denominator actually represents cumulative heat transferred to helium by fuel in the whole power plant (considering all components that use fuel).

Heat transferred to helium by fuel in the burner can be calculated by an equation:

$$\dot{Q}_{FUEL} = \dot{m}_5 \cdot (h_6 - h_5), \tag{26}$$

While heat transferred from helium to cooling water in the precooler and intercooler is:

$$\dot{Q}_{PRECOOLER} = \dot{m}_1 \cdot (h_9 - h_1), \tag{27}$$

$$\dot{Q}_{INTERCOOLER} = \dot{m}_2 \cdot (h_2 - h_3). \tag{28}$$

The energy analysis includes the regenerator and the whole power plant. Regenerator energy efficiency at each plant load will also be an important variable in the potential plant improvement investigation. According to Figure 1, regenerator energy loss (heat loss) and energy efficiency can be calculated using the following equations:

$$\dot{E}n_{L,REG} = \dot{m}_8 \cdot h_8 + \dot{m}_4 \cdot h_4 - \dot{m}_8 \cdot h_9 - \dot{m}_4 \cdot h_5, \tag{29}$$

$$\eta_{en,REG} = \frac{\dot{m}_5 \cdot h_5 - \dot{m}_4 \cdot h_4}{\dot{m}_8 \cdot h_8 - \dot{m}_9 \cdot h_9} = \frac{\dot{m}_4 \cdot (h_5 - h_4)}{\dot{m}_8 \cdot (h_8 - h_9)}, \tag{30}$$

While whole plant energy efficiency is calculated using Equation (7), the variables required in Equation (7) are defined in Equations (25) and (26). Equations for the exergy analysis of each observed plant component are presented in Table 3.

Whole plant exergy efficiency is calculated by using Equation (14), where the required variables are defined in Equations (25) and (26). The last undefined variable from Equation (14) is EC (an exergy coefficient related to heat transfer in the burner), whose value depends on the fuel type used in the combustion process. As mentioned in [38], in the burner of the Oberhausen II power plant is used coke-oven gas, whose EC is equal to 1 (based on the fuel's lower heating value) [62]. Therefore, for the whole analyzed plant, energy efficiency calculated using Equation (7) and exergy efficiency calculated using Equation (14) will be identical.

It should also be highlighted that, during whole plant efficiency calculations, the product of fuel mass flow rate and lower heating value should be placed in the denominator of Equations (7) and (14) (instead of transferred heat). For the Oberhausen II power plant, the coke-oven gas's exact composition (and consequentially lower heating value) unknown, as is the mass flow rate at any observed plant load. In the performed analyses, the product of the coke-oven gas mass flow rate and lower heating value is approximated with heat transferred to helium in the burner; therefore, heat losses in the burner are neglected.

Table 3. Exergy analysis equations of each observed plant component.

Component	Exergy Destruction	Equation
LPTC	$\dot{E}x_{D,LPTC} = \dot{m}_1 \cdot \varepsilon_1 + P_{PT,LPTC} - \dot{m}_1 \cdot \varepsilon_2$	(31)
HPTC	$\dot{E}x_{D,HPTC} = \dot{m}_3 \cdot \varepsilon_3 + P_{PT,HPTC} - \dot{m}_3 \cdot \varepsilon_4$	(32)
HPT	$\dot{E}x_{D,HPT} = \dot{m}_6 \cdot \varepsilon_6 - \dot{m}_6 \cdot \varepsilon_7 - P_{PT,HPT}$	(33)
LPT	$\dot{E}x_{D,LPT} = \dot{m}_7 \cdot \varepsilon_7 - \dot{m}_7 \cdot \varepsilon_8 - P_{PT,LPT}$	(34)
REGENERATOR	$\dot{E}x_{D,REG} = \dot{m}_8 \cdot \varepsilon_8 + \dot{m}_4 \cdot \varepsilon_4 - \dot{m}_8 \cdot \varepsilon_9 - \dot{m}_4 \cdot \varepsilon_5$	(35)
Component	**Exergy Efficiency**	**Equation**
LPTC	$\eta_{ex,LPTC} = \frac{\dot{m}_1 \cdot (\varepsilon_2 - \varepsilon_1)}{P_{PT,LPTC}}$	(36)
HPTC	$\eta_{ex,HPTC} = \frac{\dot{m}_3 \cdot (\varepsilon_4 - \varepsilon_3)}{P_{PT,HPTC}}$	(37)
HPT	$\eta_{ex,HPT} = \frac{P_{PT,HPT}}{\dot{m}_6 \cdot (\varepsilon_6 - \varepsilon_7)}$	(38)
LPT	$\eta_{ex,LPT} = \frac{P_{PT,LPT}}{\dot{m}_7 \cdot (\varepsilon_7 - \varepsilon_8)}$	(39)
REGENERATOR	$\eta_{ex,REG} = \frac{\dot{m}_4 \cdot (\varepsilon_5 - \varepsilon_4)}{\dot{m}_8 \cdot (\varepsilon_8 - \varepsilon_9)}$	(40)

4. Operating Parameters Required for the Oberhausen II Power Plant (and Plant Components) Isentropic, Energy and Exergy Analyses

Thermodynamic analysis of the Oberhausen II power plant and each observed plant component requires knowledge of helium temperature, pressure, and mass flow rate at each operating point from Figure 1 at each plant load. Helium temperature and pressure at each operating point allow the calculation of specific enthalpy and specific entropy using NIST-REFPROP 9.0 software [63]. Helium-specific exergy is calculated using Equation (9).

The exergy analysis of any system or component requires the definition of the base (dead) ambient state. In this analysis, the base ambient state is defined by the ambient pressure of 1 bar and the ambient temperature of 25 °C. The change in the ambient parameters is dominantly related to the temperature; the ambient pressure has small deviations [64].

Helium temperatures, pressures, and mass flow rates at each operating point in Figure 1 are partially derived from the literature [25,38,39] (along with my, own calculations) at each plant load. The first plant load is DESIGN LOAD—helium operating parameters at this load (Table A1, Appendix A) are not measured in the plant; they are obtained from calculations. DESIGN LOAD represents optimal power plant operating parameters that could be obtained at the nominal operating regime when all expected losses are minimal. In this load, the highest plant efficiency is expected, much higher than in the plant exploitation loads.

The other three loads of the Oberhausen II power plant are under real exploitation conditions, and helium operating parameters (pressures, temperatures, and mass flow rates) are obtained mainly from the measurements. In Table A2 (Appendix A), helium operating parameters are presented at the NOMINAL LOAD (NL), while Tables A3 and A4 (Appendix A) show helium operating parameters at two partial loads—65% of NL and 45% of NL, respectively.

5. Results of Thermodynamic Analysis and Discussion

In the Oberhausen II power plant, operating fluid (helium) leakage occurs through the gland seals of both turbocompressors (LPTC and HPTC) as well as through the gland seals of the LPT. At HPT, due to high pressures and temperatures, a certain helium mass flow rate is added to reduce leakages as well as for HPT blade cooling (Figure 3).

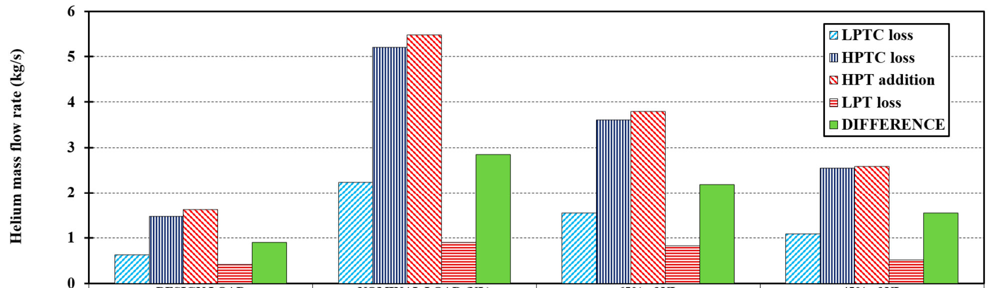

	DESIGN LOAD	NOMINAL LOAD (NL)	65% of NL	45% of NL
LPTC loss	0.63	2.23	1.55	1.09
HPTC loss	1.47	5.20	3.61	2.54
HPT addition	1.62	5.48	3.80	2.59
LPT loss	0.42	0.90	0.82	0.51
DIFFERENCE	0.90	2.85	2.18	1.55

Figure 3. Cumulative helium mass flow rate loss and addition of each turbomachine at all observed power plant loads.

Considering both turbocompressors, it is expected that at any load, cumulative helium leakage through HPTC gland seals is higher in comparison to LPTC due to higher pressures. LPT has lower cumulative helium mass flow rate leakages at all observed loads in comparison to both turbocompressors. At any plant load, cumulative helium addition in the HPT is higher than cumulative helium loss in any other turbomachine (Figure 3).

From Figure 3, it can be clearly seen that all helium leakages and helium additions are notably underestimated at the plant DESIGN LOAD even in comparison to partial loads. This fact confirms that DESIGN LOAD is actually an optimal load where the losses are minimal. It should be highlighted that, for the plant exploitation loads, cumulative helium mass flow rate losses and additions decrease during the decrease in plant load.

The DIFFERENCE shown in Figure 3 represents a helium mass flow rate that must be added to the process before the precooler at each load, Figure 1. The added mass flow rate is actually a difference between the cumulative helium mass flow rate lost at both turbocompressors and LPT and the cumulative helium mass flow rate added at HPT.

The used and produced real mechanical power of all Oberhausen II turbomachines, as well as the real useful plant mechanical power, are presented in Figure 4. At any load, it can be seen that HPTC uses almost two times more real mechanical power in comparison to LPTC. Regardless of the fact that both turbocompressors have higher helium leakage at NOMINAL LOAD in comparison to DESIGN LOAD, Figure 3), both of them use higher real mechanical power at NOMINAL LOAD. The reason for that occurrence can be seen in Appendix A, Tables A1 and A2: at NOMINAL LOAD helium mass flow rate at the entrance of each turbocompressor is notably higher than at DESIGN LOAD.

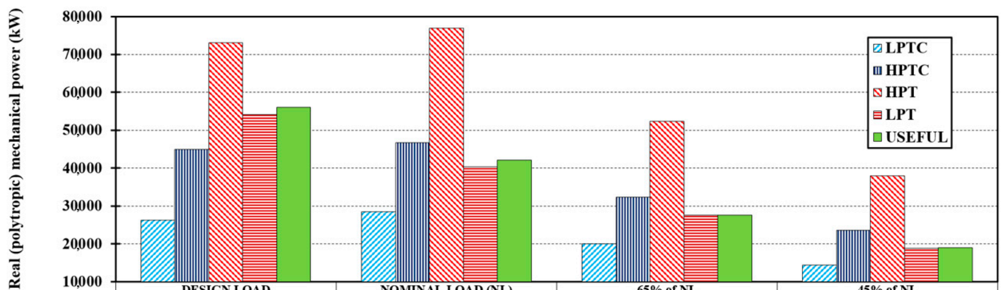

	DESIGN LOAD	NOMINAL LOAD (NL)	65% of NL	45% of NL
LPTC	26,321.95	28,478.91	20,001.97	14,367.28
HPTC	44,910.01	46,662.86	32,354.14	23,605.42
HPT	73,081.96	76,954.66	52,392.60	38,025.72
LPT	54,140.99	40,320.18	27,567.75	18,887.19
USEFUL	55,990.99	42,133.07	27,604.24	18,940.21

Figure 4. Used (turbocompressors), produced (turbines), and useful real mechanical power at all observed power plant loads.

HPT develops higher real mechanical power at NOMINAL LOAD in comparison to DESIGN LOAD due to prolonged expansion (lower helium temperature and pressure at the HPT outlet). Unlike HPT, LPT develops the highest real mechanical power at DESIGN LOAD (in comparison to NOMINAL LOAD) due to its much longer expansion at DESIGN LOAD regardless of the fact that at NOMINAL LOAD LPT passes a higher helium mass flow rate. At any observed plant load in exploitation, HPT produces almost two times more real mechanical power in comparison to LPT.

Useful real mechanical power is applied to the electric generator drive and is obtained when the real mechanical power produced by both turbines is subtracted from the real mechanical power used by both turbocompressors. Useful real mechanical power is the highest at DESIGN LOAD and equals almost 56 MW (Figure 4). At each observed load, the HPT produces sufficient mechanical power for both turbocompressor drives (the remaining real mechanical power produced by the HPT is delivered to an electric generator through the gearbox, Figure 1).

The isentropic efficiency of each Oberhausen II turbomachine, at all analyzed plant loads, is presented in Figure 5.

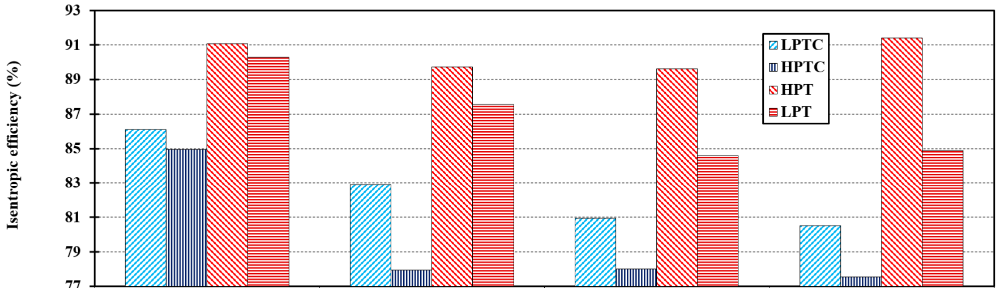

	DESIGN LOAD	NOMINAL LOAD (NL)	65% of NL	45% of NL
LPTC	86.10	82.90	80.94	80.51
HPTC	84.95	77.93	78.00	77.56
HPT	91.08	89.72	89.62	91.39
LPT	90.28	87.57	84.58	84.88

Figure 5. Isentropic efficiency of each turbomachine (turbocompressor and turbine) at all observed power plant loads.

At each load, LPTC has higher isentropic efficiency in comparison to HPTC due to lower isentropic losses. At plant loads in exploitation, HPTC isentropic efficiency did not exceed 78% and is lower in comparison to all other turbomachines. For both turbocompressors, isentropic efficiency is notably higher at DESIGN LOAD in comparison to all exploitation loads (for the HPTC mentioned, the difference is 7% or higher), which confirms underestimation of isentropic losses and overestimation of isentropic efficiencies in design conditions. Both turbines (HPT and LPT) have higher isentropic efficiencies in comparison to turbocompressors at each load. HPT has the highest isentropic efficiency of all turbomachines at all plant loads (around 90% or higher).

For many heat exchangers, energy analysis is not recommended because it can be highly dependable in terms of measurement accuracy and precision. In such heat exchangers, a slight measurement error can lead to unreasonable energy analysis variables (negative energy loss and energy efficiency higher than 100%) [43].

The regenerator used in the Oberhausen II power plant is not highly sensitive to measurement accuracy and precision, but as for other heat exchangers, high energy efficiencies and low energy losses (low heat losses) can be expected. The regenerator has the highest energy efficiency, equal to 98.25%, at the DESIGN LOAD, while in exploitation its energy efficiency did not exceed 98% (the highest regenerator energy efficiency in plant exploitation can be seen at NOMINAL LOAD, equal to 97.80%), Figure 6.

Heat transferred to helium by fuel in the burner at all observed power plant loads is presented in Figure 7. As can be seen from Figure 7, heat transferred to helium by fuel in the burner is the highest at the DESIGN LOAD (almost 146 MW), while observing exploitation loads, the highest value of this variable is detected at NOMINAL LOAD.

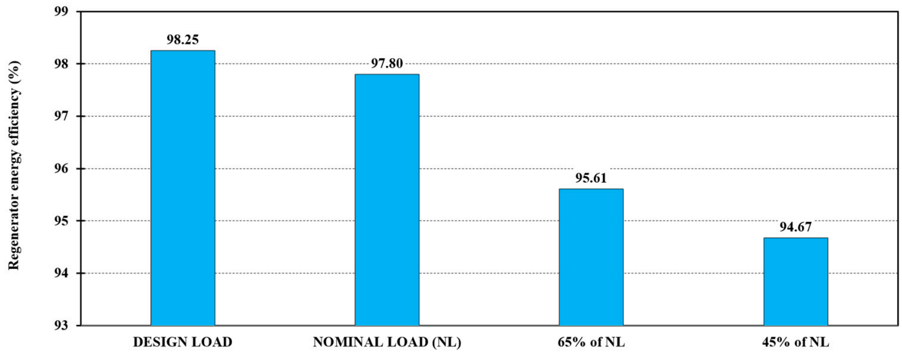

Figure 6. The regenerator energy efficiency at all observed power plant loads.

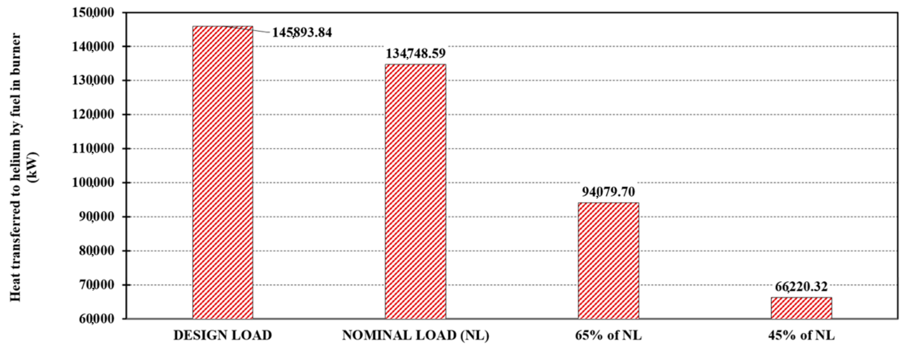

Figure 7. Heat transferred to helium by fuel in the burner at all observed power plant loads.

Heat transferred to helium by fuel in the burner is an important variable for the whole plant efficiency calculation. As evident from Equations (7) and (14), heat transferred to helium by fuel in the burner is placed in the denominator of both equations; therefore, the reduction of this variable can notably increase the whole plant's efficiency.

The Exergy destruction of each observed power plant component at all analyzed loads is presented in Figure 8. Considering all turbomachines, it can be concluded from Figure 8 that both turbines (HPT and LPT) have lower exergy destruction in comparison to both turbocompressors (LPTC and HPTC) at each plant load. At almost all plant loads (an exception can be seen at 45% of NL), LPT has lower exergy destruction than HPT, while HPTC at all plant loads has notably higher exergy destruction than LPTC. LPT has the lowest, while HPTC has the highest exergy destruction of all turbomachines. At all observed loads, regenerator exergy destruction is higher in comparison to any turbomachine.

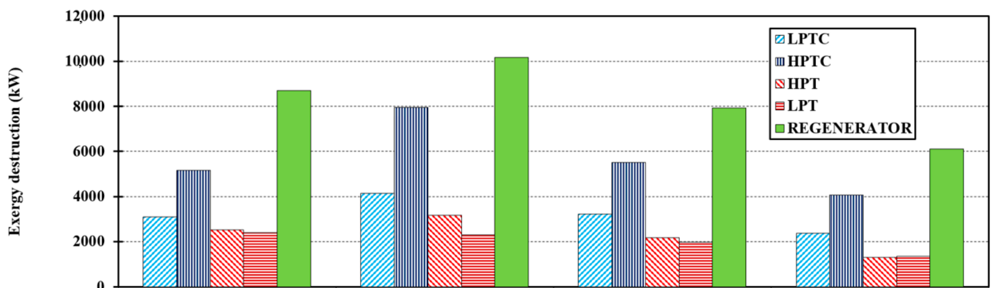

	DESIGN LOAD	NOMINAL LOAD (NL)	65% of NL	45% of NL
LPTC	3079.40	4135.22	3227.56	2361.74
HPTC	5160.79	7962.03	5496.91	4062.98
HPT	2506.68	3159.75	2176.20	1286.43
LPT	2382.75	2288.37	1974.91	1341.28
REGENERATOR	8691.12	10,182.14	7918.43	6107.38

Figure 8. Exergy destruction of the analyzed power plant components at all observed loads.

The exergy efficiency of each observed Oberhausen II component at all loads is presented in Figure 9. At DESIGN LOAD exergy efficiencies of all observed components are notably overestimated in comparison to real exploitation conditions. That overestimation is the highest for turbocompressors, especially HPTC, whose exergy efficiency at DESIGN LOAD is 5.5% higher than the highest exergy efficiency in exploitation.

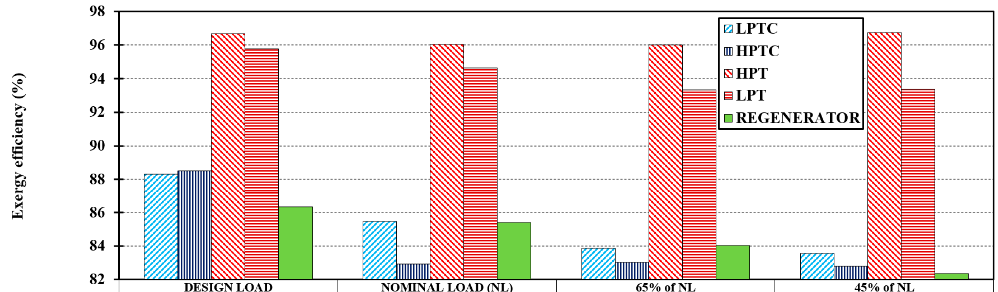

	DESIGN LOAD	NOMINAL LOAD (NL)	65% of NL	45% of NL
LPTC	88.30	85.48	83.86	83.56
HPTC	88.51	82.94	83.01	82.79
HPT	96.68	96.06	96.01	96.73
LPT	95.78	94.63	93.32	93.37
REGENERATOR	86.35	85.39	84.02	82.37

Figure 9. Exergy efficiency of the analyzed power plant components at all observed loads.

Considering all plant loads in exploitation (NL, 65% of NL, and 45% of NL), it is clear that LPTC has higher exergy efficiencies in comparison to HPTC due to lower exergy destruction, Figures 8 and 9. Both turbines (HPT and LPT) have notably higher exergy efficiency in comparison to turbocompressors (higher than 93%) at any plant load. HPT has the highest, while HPTC has the lowest exergy efficiency of all turbomachines, at all observed exploitation loads.

Due to additional losses related to the ambient, regenerator exergy efficiencies are not as high as energy efficiencies (Figures 6 and 9); however, the obtained regenerator exergy efficiencies are still acceptable (higher than 82% at all plant loads).

For all observed Oberhausen II power plant components, analysis is performed related to the ambient temperature change's influence on exergy variables. During the ambient temperature variation, the ambient pressure remains constant and the same as at the base ambient state (1 bar). Ambient temperature varies from 5 °C up to 45 °C.

Figure 10 presents the energy efficiency change of all analyzed power plant components during the ambient temperature variation at two observed loads: NL and 45% of NL. The obtained trends and conclusions are valid also for other power plant loads.

The ambient temperature change has a low, almost negligible influence on the exergy destruction and exergy efficiency of both turbines. The ambient temperature change of 10 °C results in an exergy efficiency change of both turbines equal to 0.2% or lower, regardless of the observed load. The same trends can be found in [65] for a steam turbine and in [17] for an open-cycle gas turbine, so for all turbines it can be concluded that they are less influenced by the ambient temperature change.

Turbocompressors are more influenced by ambient temperature changes in comparison to turbines. The ambient temperature change of 10 °C results in both turbocompressors' energy efficiency changing by between 0.5% and 0.6%, regardless of the observed load. Therefore, turbocompressors are around three times more sensitive to ambient temperature changes in comparison to turbines.

The regenerator is a component (of all observed components) whose exergy variables are the most sensitive to ambient temperature changes (Figure 10). Such an occurrence can be expected not only for the regenerator but also for heat exchangers in general [65]. The ambient temperature change of 10 °C results in a regenerator exergy efficiency change of around 0.8% or more, regardless of the observed load.

According to Equations (7) and (14) and considering that for coke-oven gas used in the burner, the exergy coefficient (EC) is equal to 1, the results of the whole plant energy and exergy efficiency will be the same at each analyzed plant load (Figure 11). Due to this fact, both efficiencies will be called simply "plant efficiency." The whole plant efficiency is calculated on the basis of electric power production only (due to unknown cooling water operating parameters).

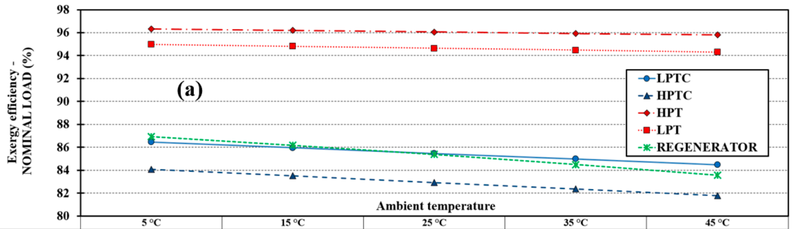

	5 °C	15 °C	25 °C	35 °C	45 °C
LPTC	86.45	85.96	85.48	85.00	84.48
HPTC	84.09	83.53	82.94	82.38	81.81
HPT	96.31	96.19	96.06	95.92	95.80
LPT	94.99	94.81	94.63	94.47	94.31
REGENERATOR	86.93	86.17	85.39	84.50	83.57

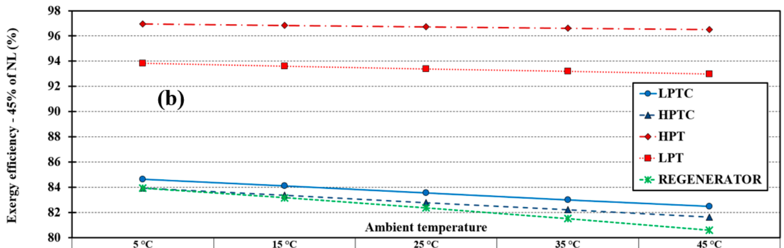

	5 °C	15 °C	25 °C	35 °C	45 °C
LPTC	84.64	84.10	83.56	83.00	82.47
HPTC	83.93	83.36	82.79	82.21	81.64
HPT	96.93	96.83	96.73	96.62	96.52
LPT	93.82	93.61	93.37	93.19	92.97
REGENERATOR	83.92	83.17	82.37	81.52	80.61

Figure 10. The energy efficiency change of all analyzed power plant components during the ambient temperature variation for (**a**) NOMINAL LOAD and (**b**) 45% of NL.

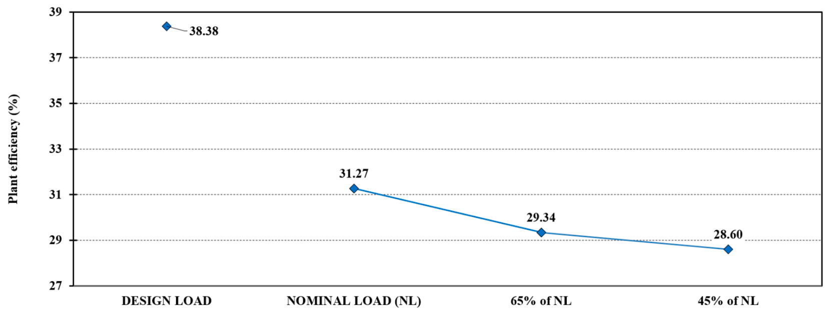

Figure 11. Whole plant efficiency at all observed loads.

As highlighted before for the power plant components, DESIGN LOAD represents optimal operating conditions, and the whole plant efficiency is expected to be much higher in comparison to any exploitation load. Whole plant efficiency at DESIGN LOAD is equal to 38.38%, and it can be used as a guideline during plant improvement or optimization.

Considering exploitation loads (connected with the line in Figure 11), the highest efficiency of the whole plant is calculated at NOMINAL LOAD (31.27%), and it continuously decreases during the decrease in plant load (and vice versa). In the literature [38], it can be found that for Oberhausen II NOMINAL LOAD in exploitation, the obtained plant efficiency is equal to 31.3% (heat flow transferred to consumers is not considered); therefore, it can be concluded that the adopted assumptions and simplifications did not notably ruin general power plant performance data.

The literature [19] offers theoretical considerations that highlight that closed-cycle gas turbine power plants have a much lower efficiency drop at partial loads in comparison to open cycle gas turbine power plants. So far, the existing literature has not offered exact confirmation of these considerations. An efficiency comparison of a closed-cycle gas turbine power plant (Oberhausen II) and three different open-cycle gas turbine power plants at various loads is presented in Figure 12.

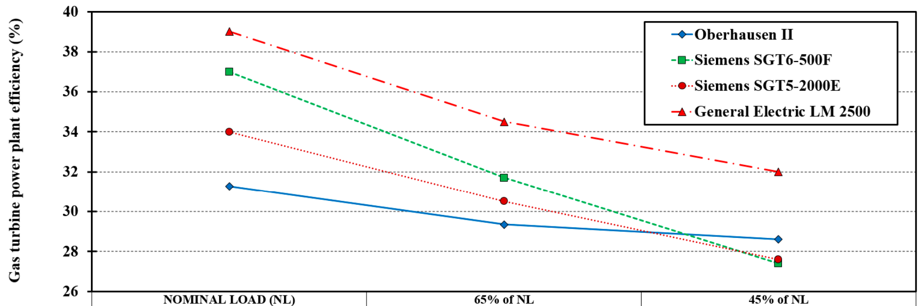

	NOMINAL LOAD (NL)	65% of NL	45% of NL
Oberhausen II	31.27	29.34	28.60
Siemens SGT6-500F	37.00	31.70	27.40
Siemens SGT5-2000E	34.00	30.50	27.60
General Electric LM 2500	39.00	34.50	32.00

Figure 12. Efficiency comparison of several gas turbine power plants at various loads—only Oberhausen II is a closed-cycle gas turbine power plant; others are open cycle gas turbine power plants.

Figure 12 exactly confirms theoretical considerations from the literature—the decrease in efficiency of a closed-cycle gas turbine power plant at partial loads is much lower in comparison to any open-cycle gas turbine power plant. A decrease in load from NOMINAL LOAD to 45% of NL results in an Oberhausen II closed-cycle gas turbine power plant efficiency decrease of only 2.67%, while between the same loads, the efficiency decrease of the Siemens SGT6-500F open-cycle gas turbine power plant [66] is 9.6%, that of the Siemens SGT5-2000E open-cycle gas turbine power plant [67,68] is 6.4%, and that of the General Electric LM 2500 open-cycle gas turbine power plant [69] is 7%. It can be concluded that the efficiency decrease of an open-cycle gas turbine power plant during load decrease is approximately two and a half or more times higher in comparison to a closed-cycle gas turbine power plant. Therefore, closed-cycle gas turbine power plants can be recommended for the application at partial loads.

6. Improvement Potential of Oberhausen II Power Plant by Increasing Components Isentropic or Energy Efficiency

In this part of the research, the influence of each observed Oberhausen II power plant component is isentropic or energy efficiency increase, in relation to the whole plant efficiency increase. The main aim of this investigation was to detect the component (or more of them) whose improvement would result in the highest increase in whole plant efficiency at all observed plant loads.

The whole plant efficiency is calculated according to the following equation:

$$\eta_{WP} = \frac{P_{PT,USEFUL}}{\dot{Q}_{FUEL}} = \frac{P_{PT,HPT} + P_{PT,LPT} - P_{PT,HPTC} - P_{PT,LPTC}}{\dot{Q}_{BURNER}}. \quad (41)$$

It should be highlighted that during any observed plant component isentropic or energy efficiency increase, the change in operating parameters is simultaneously considered, which will influence any variable from Equation (41).

The influence of each turbomachine isentropic efficiency increase on the whole plant efficiency at all observed plant loads is presented in Figure 13.

From Figure 13, it can be seen that the increase in isentropic efficiency of any turbomachine will increase whole plant efficiency, but the intensity of the increase is not the same for all turbomachines. Turbomachines whose slope of the curve is the steepest during the increase in isentropic efficiency will increase the whole plant's efficiency the most (and vice versa). Figure 13 shows that HPT has the steepest slope of the curve at all plant loads; therefore, the increase in HPT isentropic efficiency will increase the whole plant efficiency more than any other turbomachine. Simultaneously, at all observed plant loads, LPTC has the least steep slope of the curve.

Isentropic and exergy analyses show that HPT has notably higher efficiencies in comparison to all other turbomachines from the observed plant (Figures 5 and 9), so it is interesting that a further increase in HPT isentropic efficiency will be the most beneficial to the whole plant efficiency increase at all loads. An increase in HPTC isentropic efficiency, which is the component with the lowest efficiencies (Figures 5 and 9), will not be the most beneficial to the whole plant's efficiency at any load.

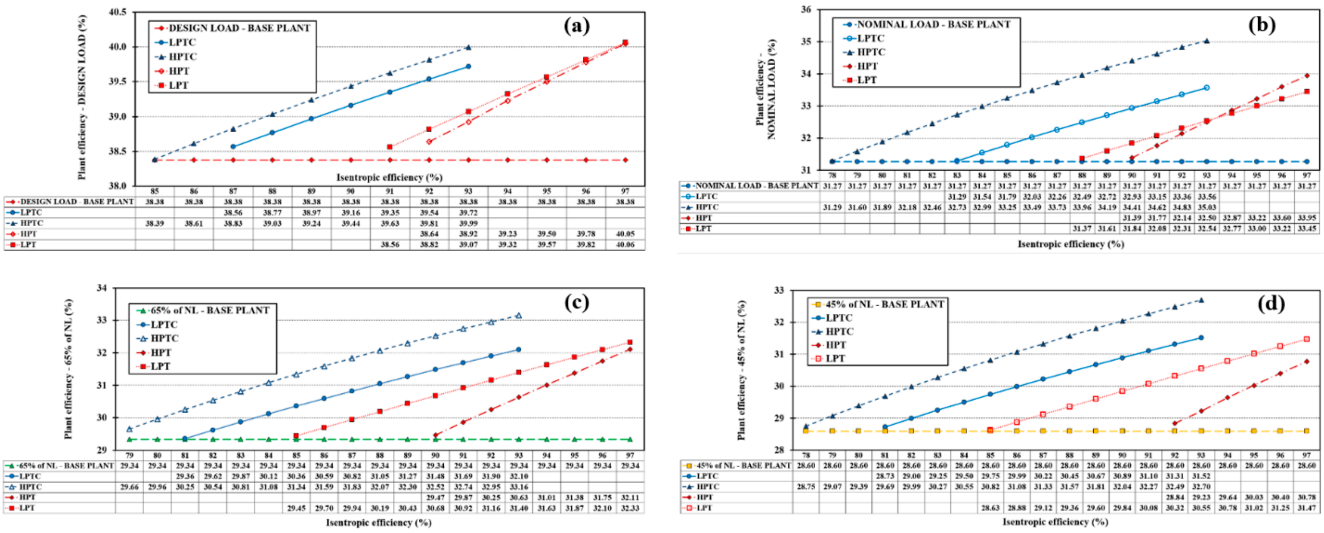

Figure 13. The influence of each turbomachine isentropic efficiency increase on the whole plant efficiency at: (**a**) DESIGN LOAD; (**b**) NOMINAL LOAD; (**c**) 65% of NL; (**d**) 45% of NL.

The final conclusion derived from this part of the analysis is that improvements to turbomachines, which have the lowest efficiencies, do not have to be the most influential on the whole plant's efficiency (for turbomachines from the Oberhausen II power plant, this is a totally opposite conclusion).

A clearer presentation of each observed Oberhausen II component improvement influence on the whole plant efficiency is presented in Figure 14 through the average values.

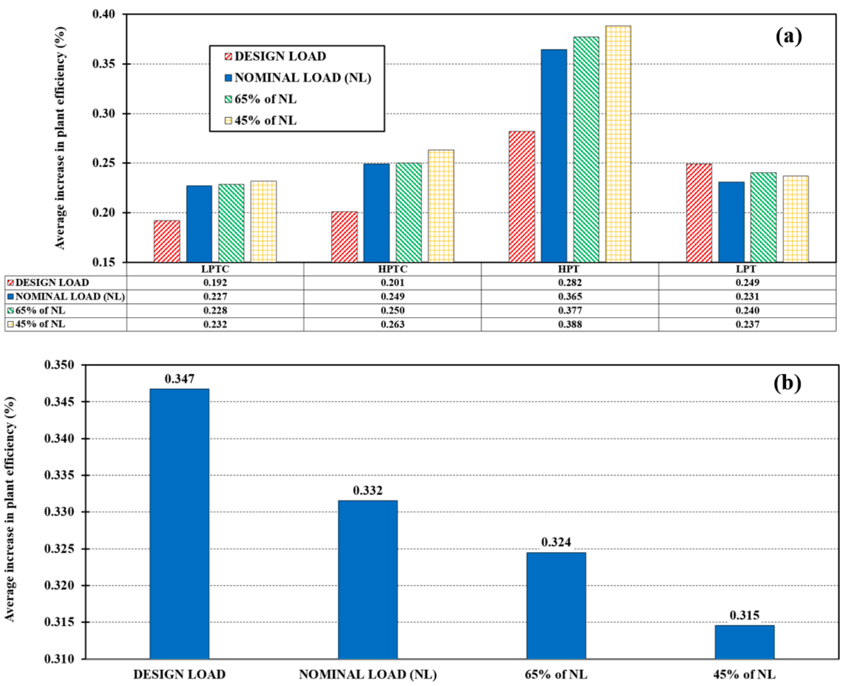

Figure 14. Whole plant average efficiency increase at all observed loads during the increase in (**a**) each turbomachine isentropic efficiency of 1% and (**b**) regenerator energy efficiency of 1%.

Previously derived conclusions related to the turbomachines are clearly visible in Figure 14a. HPT isentropic efficiency increases of 1% will result in an average increase in whole plant efficiency of more than 0.35% at all loads in exploitation. Also, the HPTC isentropic efficiency increase of 1% will result in a slightly higher whole plant average efficiency increase in comparison to the increase in LPT isentropic efficiency of 1% at all plant loads in exploitation (NL, 65% of NL, and 45% of NL). Figure 14b shows the average increase in whole plant efficiency at all observed loads during the increase in regenerator energy efficiency. An increase in the regenerator energy efficiency of 1% will result in a whole plant average efficiency increase of 0.31% or more at all observed loads.

7. Improvement Potential of Oberhausen II Power Plant by Involving an Additional Heater (AH) in the Plant Operation

In this paper, the possibility of additional heater (AH) implementation in the Oberhausen II power plant operation is also analyzed. It will be analyzed how the AH implementation influences the whole plant's efficiency in the ideal scenario (without helium pressure drop in the AH) and in the real scenario (with helium pressure drop in the AH). The general scheme of the Oberhausen II plant with its implemented AH is shown in Figure 15.

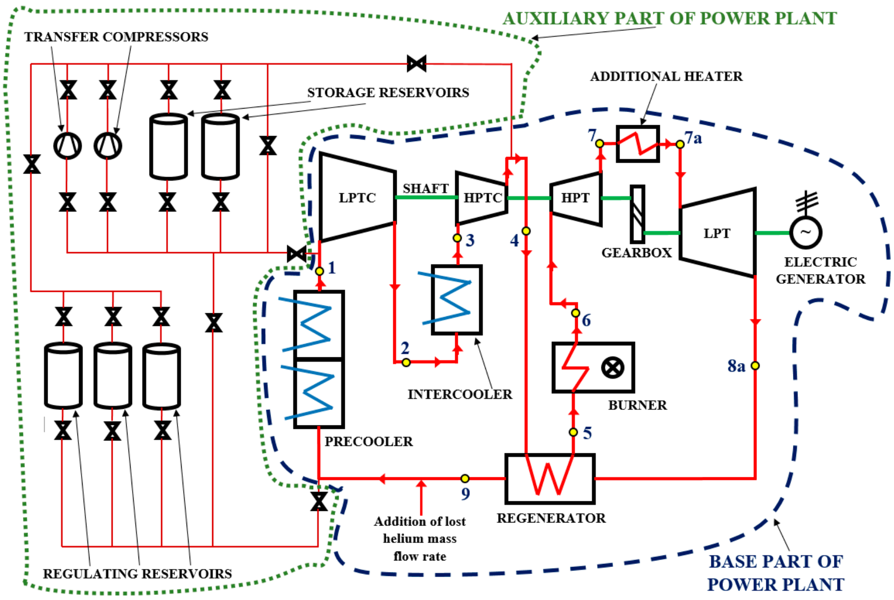

Figure 15. General scheme of the Oberhausen II power plant with implemented additional heater (AH) along with marked operating points required for the improvement potential analysis.

The helium heating process in the AH and expansion through both turbines (HPT and LPT) in h-s diagrams are presented in Figure 16a for an ideal scenario without helium pressure drop in the AH (operating point 7a has the same pressure as operating point 7) and in Figure 16b for a real scenario with helium pressure drop in the AH (operating point 7a has a lower pressure than operating point 7). At all observed Oberhausen II loads, the helium average pressure drop in the burner between the inlet and outlet is equal to 5.5% (close to 6% if only the exploitation loads are observed). So, it is reasonable to expect that the helium pressure drop in a real AH operation will be around 5% (however, the whole range of helium pressure drop in the AH from 3% up to 5% has been investigated). It is assumed that the AH uses the same fuel as the burner (coke-oven gas), and the helium outlet temperatures from the AH vary between 630 °C and 750 °C (in steps of 10 °C). As the helium temperature at the burner outlet (operating point 6, Figure 15) did not exceed 750 °C at any observed load, it will not be reasonable to expect higher helium temperatures at the AH outlet.

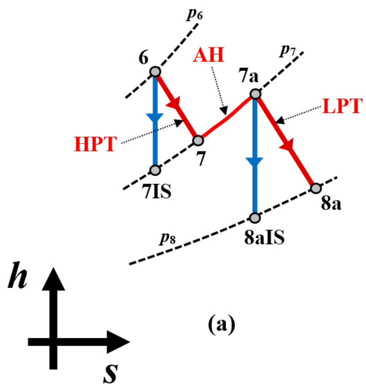

Figure 16. Specific enthalpy—specific entropy (h-s) diagrams for a process with AH included: (**a**) ideal scenario without helium pressure drop in the AH; (**b**) real scenario with helium pressure drop in the AH.

As the AH uses fuel, the whole plant efficiency with an implemented AH can be calculated by the following equation:

$$\eta_{WP} = \frac{P_{PT,USEFUL}}{\dot{Q}_{FUEL}} = \frac{P_{PT,HPT} + P_{PT,LPT} - P_{PT,HPTC} - P_{PT,LPTC}}{\dot{Q}_{BURNER} + \dot{Q}_{AH}}. \tag{42}$$

In the above equation, the real mechanical power of each component is calculated by using equations from Table 2 (the only modification is related to the LPT, where the difference in helium specific enthalpies is related to operating points 7a and 8a, according to markings from Figures 15 and 16). The heat transferred to helium by fuel in the burner ($\dot{Q}_{BURNER}$) is calculated by using Equation (26), while the heat transferred to helium by fuel in the AH ($\dot{Q}_{AH}$) is calculated according to the following equation (markings are related to Figures 15 and 16):

$$\dot{Q}_{AH} = \dot{m}_7 \cdot (h_{7a} - h_7). \tag{43}$$

7.1. Involving an Additional Heater (AH) in the Plant Operation—Ideal Scenario

Figure 17 shows an increase in whole plant efficiency if the ideal AH process is implemented in the plant (for a selected range of helium temperatures at the AH outlet). Figure 17a presents the increase in plant efficiency at DESIGN LOAD and NOMINAL LOAD, while Figure 17b shows the increase in plant efficiency at 65% of NL and 45% of NL after the ideal AH implementation. For all helium temperatures at the AH outlet, at each load, implementation of the ideal AH process increases overall plant efficiency (the plant efficiency increase is higher as the helium temperature at the AH outlet increases).

In an ideal AH process without helium pressure drop, an increase in the helium temperature at the AH outlet from 630 °C up to 750 °C will increase whole plant efficiency between 1.11% and 3.75% at DESIGN LOAD, between 1.29% and 3.58% at NL, between 1.07% and 3.12% at 65% of NL, and between 1.17% and 3.13% at 45% of NL, respectively, in comparison to the base process (base plant), Figure 17.

The presented results lead to the conclusion that, if the helium pressure drop in the AH is neglected, the additional heating process can be notably beneficial to the whole plant's efficiency, especially with as high a helium temperature as possible at the AH outlet.

7.2. Involving an Additional Heater (AH) in the Plant Operation—Real Scenario

Figure 18 presents the whole plant efficiency change when the helium pressure drop in AH is equal to 3%, 4%, or 5% at all observed plant loads. The change in plant efficiency with AH implemented in real operation is compared to the base process at each load.

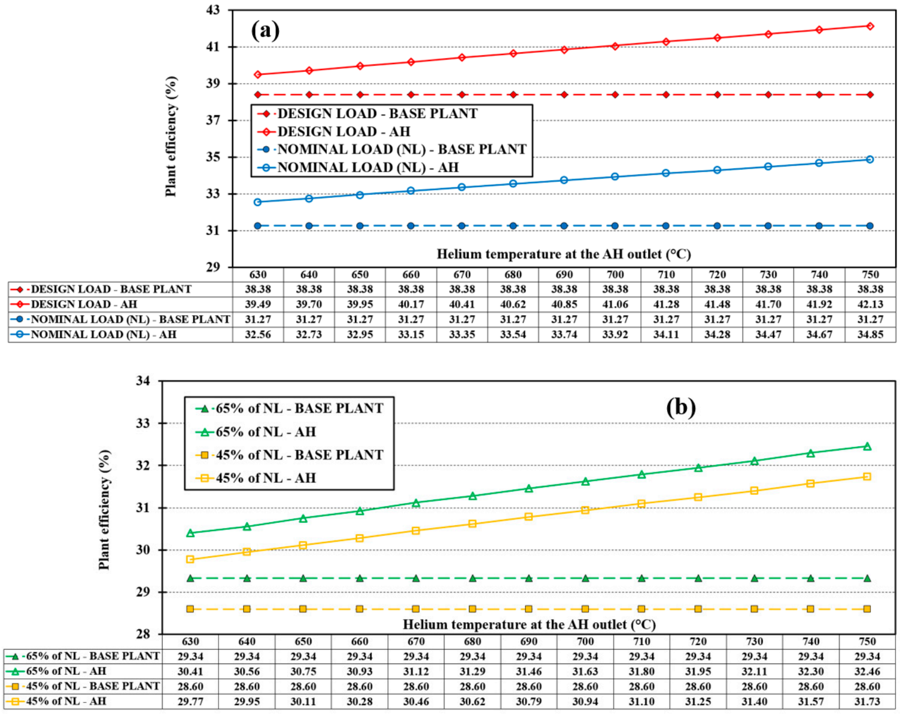

	630	640	650	660	670	680	690	700	710	720	730	740	750
DESIGN LOAD - BASE PLANT	38.38	38.38	38.38	38.38	38.38	38.38	38.38	38.38	38.38	38.38	38.38	38.38	38.38
DESIGN LOAD - AH	39.49	39.70	39.95	40.17	40.41	40.62	40.85	41.06	41.28	41.48	41.70	41.92	42.13
NOMINAL LOAD (NL) - BASE PLANT	31.27	31.27	31.27	31.27	31.27	31.27	31.27	31.27	31.27	31.27	31.27	31.27	31.27
NOMINAL LOAD (NL) - AH	32.56	32.73	32.95	33.15	33.35	33.54	33.74	33.92	34.11	34.28	34.47	34.67	34.85

	630	640	650	660	670	680	690	700	710	720	730	740	750
65% of NL - BASE PLANT	29.34	29.34	29.34	29.34	29.34	29.34	29.34	29.34	29.34	29.34	29.34	29.34	29.34
65% of NL - AH	30.41	30.56	30.75	30.93	31.12	31.29	31.46	31.63	31.80	31.95	32.11	32.30	32.46
45% of NL - BASE PLANT	28.60	28.60	28.60	28.60	28.60	28.60	28.60	28.60	28.60	28.60	28.60	28.60	28.60
45% of NL - AH	29.77	29.95	30.11	30.28	30.46	30.62	30.79	30.94	31.10	31.25	31.40	31.57	31.73

Figure 17. The AH involvement in the power plant structure—ideal scenario: (**a**) Increase in power plant efficiency at DESIGN LOAD and NOMINAL LOAD; (**b**) Increase in power plant efficiency at 65% of NL and 45% of NL.

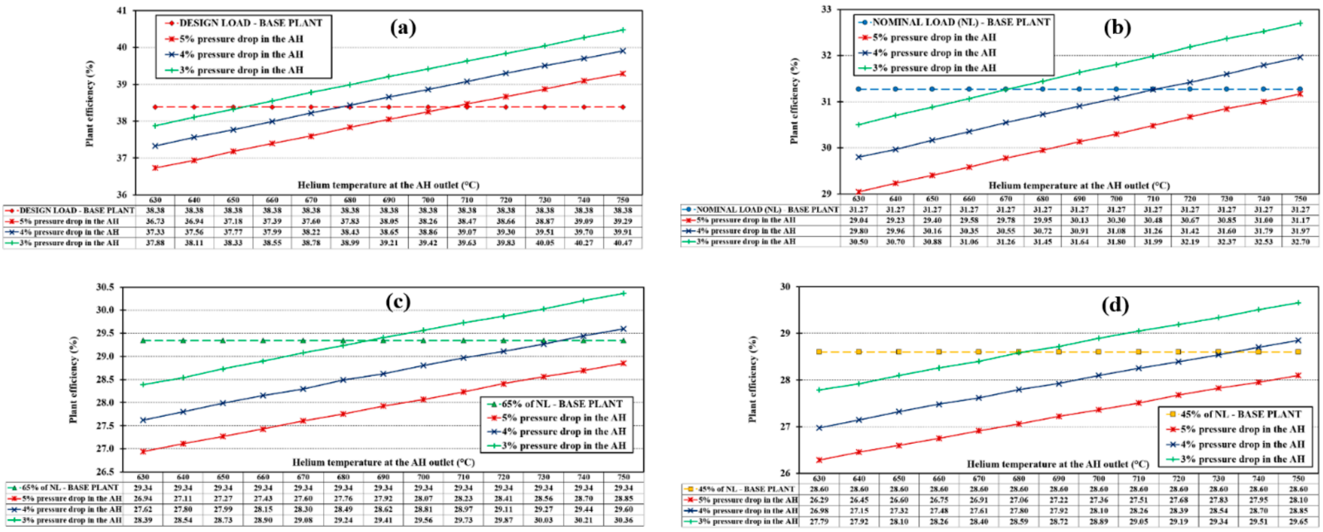

	630	640	650	660	670	680	690	700	710	720	730	740	750
DESIGN LOAD - BASE PLANT	38.38	38.38	38.38	38.38	38.38	38.38	38.38	38.38	38.38	38.38	38.38	38.38	38.38
5% pressure drop in the AH	36.73	36.94	37.18	37.39	37.60	37.83	38.05	38.26	38.47	38.66	38.87	39.09	39.29
4% pressure drop in the AH	37.33	37.56	37.77	37.99	38.22	38.43	38.65	38.86	39.07	39.30	39.51	39.70	39.91
3% pressure drop in the AH	37.88	38.11	38.33	38.55	38.78	38.99	39.21	39.42	39.63	39.83	40.05	40.27	40.47

	630	640	650	660	670	680	690	700	710	720	730	740	750
NOMINAL LOAD (NL) - BASE PLANT	31.27	31.27	31.27	31.27	31.27	31.27	31.27	31.27	31.27	31.27	31.27	31.27	31.27
5% pressure drop in the AH	29.04	29.23	29.40	29.58	29.78	29.95	30.13	30.30	30.48	30.67	30.85	31.00	31.17
4% pressure drop in the AH	29.80	29.96	30.16	30.35	30.55	30.72	30.91	31.08	31.26	31.42	31.60	31.79	31.97
3% pressure drop in the AH	30.50	30.70	30.88	31.06	31.26	31.45	31.64	31.80	31.99	32.19	32.37	32.53	32.70

	630	640	650	660	670	680	690	700	710	720	730	740	750
65% of NL - BASE PLANT	29.34	29.34	29.34	29.34	29.34	29.34	29.34	29.34	29.34	29.34	29.34	29.34	29.34
5% pressure drop in the AH	26.94	27.11	27.27	27.43	27.60	27.76	27.92	28.07	28.23	28.41	28.56	28.70	28.85
4% pressure drop in the AH	27.62	27.80	27.99	28.15	28.30	28.49	28.62	28.81	28.97	29.11	29.27	29.44	29.60
3% pressure drop in the AH	28.39	28.54	28.73	28.90	29.08	29.24	29.41	29.56	29.73	29.87	30.03	30.21	30.36

	630	640	650	660	670	680	690	700	710	720	730	740	750
45% of NL - BASE PLANT	28.60	28.60	28.60	28.60	28.60	28.60	28.60	28.60	28.60	28.60	28.60	28.60	28.60
5% pressure drop in the AH	26.29	26.45	26.60	26.75	26.91	27.06	27.22	27.36	27.51	27.68	27.83	27.95	28.10
4% pressure drop in the AH	26.98	27.15	27.32	27.48	27.61	27.80	27.92	28.10	28.26	28.39	28.54	28.70	28.85
3% pressure drop in the AH	27.79	27.92	28.10	28.26	28.40	28.59	28.72	28.89	29.05	29.19	29.34	29.51	29.65

Figure 18. The AH involvement in the power plant structure—real scenario—increase in power plant efficiency at: (**a**) DESIGN LOAD; (**b**) NOMINAL LOAD; (**c**) 65% of NL; (**d**) 45% of NL.

Only at DESIGN LOAD, which represents an optimal plant operating regime, can the whole plant's efficiency be higher in comparison to the base process for all observed helium pressure drops in the AH. However, even at the lowest DESIGN LOAD possible, helium temperatures will be required at the AH outlet to achieve a reasonable whole plant efficiency increase (in comparison to the base process).

In real operating conditions, by assuming a reasonable helium pressure drop in the AH of 5%, additional heating processes will not be able to achieve a power plant efficiency increase in comparison to the base process for all observed exploitation loads. Even if the helium pressure drop in the AH is equal to 4%, in plant exploitation, a reasonable plant efficiency increase (in comparison to the base process) cannot be achieved for the highest observed helium temperatures at the AH outlet. Additional heating processes can be beneficial for unreasonably low helium pressure drops in the AH or for unreasonably high helium temperatures at the AH outlet. Finally, it can be concluded that Oberhausen II power plant in real operating conditions cannot be improved by the implementation of additional heating processes at all observed exploitation loads.

8. Conclusions

In this research, isentropic, energy, and exergy analyses are performed on Oberhausen II (a helium closed cycle gas turbine power plant) and the dominant plant components at four loads (the design load and three loads during the plant's exploitation). All loads are considered helium leakages and additions to each turbomachine. Obtained efficiencies, losses, and destructions present a good insight into the operation of each observed component and the whole power plant at various loads. The influence of the ambient temperature change on exergy analysis variables is presented for all observed plant components. Oberhausen II power plant efficiencies at various loads are directly compared to those of three open-cycle gas turbine power plants. It is investigated the improvement potential of the Oberhausen II power plant (potential of the whole plant efficiency increase) in two different ways: by increasing each observed component isentropic or energy efficiency and by involving an additional heater in the plant operation. The most important conclusions are:

- In the observed plant, HPT is the dominant mechanical power producer, while HPTC is the dominant mechanical power consumer, regardless of the observed load.
- Both turbines (HPT and LPT) have notably higher isentropic and exergy efficiencies (around 85% or higher) in comparison to both turbocompressors (LPTC and HPTC) at each plant load.
- HPT has the highest isentropic and exergy efficiencies of all turbomachines, while HPTC is detected as the most problematic turbomachine with the lowest isentropic and exergy efficiencies at all loads.
- Regenerator shows very good operation performance (its energy efficiency is higher than 94% and exergy efficiency is higher than 82%) at all plant loads. Considering all observed power plant components, the exergy variables of the regenerator are the most sensitive to ambient temperature change.
- DESIGN LOAD represents optimal operating conditions at which the whole plant efficiency is equal to 38.38%. Considering power plant loads in real exploitation, the highest efficiency of the whole plant is obtained at NOMINAL LOAD (31.27%).
- The decrease in open cycle gas turbine power plant efficiency at partial loads is approximately two and a half or more times higher than for the closed cycle gas turbine power plant.
- Regardless of the fact that HPTC has the lowest efficiencies of all turbomachines, a further increase in HPT isentropic efficiency (HPT has the highest efficiencies of all turbomachines) will be the most beneficial to the whole plant at all observed loads.
- An increase in the HPT isentropic efficiency of 1% will result in an average increase in whole plant efficiency of more than 0.35% at all loads in the plant's exploitation. Regenerator improvement will also have a notable influence on the observed power plant performance—an increase in the regenerator energy efficiency of 1% will result in an average increase in whole plant efficiency of 0.31% or more at all plant loads.
- In real operating conditions, by assuming a reasonable helium pressure drop of 5% in the additional heater, the additional heating process will not be able to increase plant efficiency at all loads in exploitation (in comparison to the process without additional heating). Therefore, the Oberhausen II power plant cannot be improved by the implementation of the additional heating process.

Further research related to the Oberhausen II power plant will be based on optimization possibilities investigated using artificial intelligence methods and techniques. In addition, the results presented in this analysis will serve as a baseline for further research on closed-cycle gas turbine power plants, their processes, performances, and characteristics.

Author Contributions: Conceptualization, V.M., I.P. and M.J.; methodology, V.M. and I.P.; software, V.M. and M.J.; validation, I.P. and M.J.; formal analysis, V.M. and J.P.-O.; investigation, V.M., I.P. and M.J.; resources, V.M.; data curation, I.P. and M.J.; writing—original draft preparation, V.M. and I.P.; writing—review and editing, M.J. and J.P.-O.; visualization, V.M., I.P. and M.J.; supervision, J.P.-O.; All authors have read and agreed to the published version of the manuscript.

Funding: This research received no external funding.

Data Availability Statement: Not applicable.

Acknowledgments: This research has been supported by the Croatian Science Foundation under the project IP-2018-01-3739, University of Rijeka scientific grant uniri-tehnic-18-18-1146 and the University of Rijeka scientific grant uniri-tehnic-18-14.

Conflicts of Interest: The authors declare no conflict of interest.

Nomenclature

Abbreviations	
AH	Additional Heater
CHP	Combined Heat and Power
CO_2	Carbon Dioxide
EC	Exergy Coefficient
HPT	High Pressure Turbine
HPTC	High Pressure Turbocompressor
LPT	Low Pressure Turbine
LPTC	Low Pressure Turbocompressor
NL	Nominal Load
Latin symbols	
h	specific enthalpy, kJ/kg
$\dot{m}$	mass flow rate, kg/s
P	mechanical power, kW
$\dot{Q}$	heat energy transfer, kW
s	specific entropy, kJ/kg·K
T	temperature, K or °C
$\dot{X}_{heat}$	heat exergy transfer, kW
Greek symbols	
ε	specific exergy, kJ/kg
η	efficiency, %
Subscripts	
0	base (dead) ambient state
D	destruction
en	energy
ex	exergy
HE	Heat Exchanger
in	inlet (input)
IS	isentropic
L	loss (heat loss)
out	outlet (output)
PT	polytropic
REG	regenerator
WP	Whole Plant

Appendix A

Helium operating parameters at each observed plant load (operating point numeration refers to Figure 1) are calculated for the base ambient state.

Table A1. Oberhausen II operating parameters at DESIGN LOAD.

Operating Point	Mass Flow Rate (kg/s)	Temperature (°C)	Pressure (bar)	Specific Enthalpy (kJ/kg)	Specific Entropy (kJ/kg·K)	Specific Exergy (kJ/kg)	Isentropic Specific Enthalpy (kJ/kg)
1	86.50	25.0	10.49	1556.9	23.152	1458.4	-
2	85.87	83.3	15.48	1861.2	23.272	1727.1	1818.9
3	85.87	25.0	15.38	1558.4	22.358	1696.8	-
4	84.40	124.9	28.76	2081.4	22.560	2159.7	2002.7
5	84.40	417.0	28.16	3597.8	25.461	2811.1	-
6	84.40	750.0	27.00	5326.4	27.592	3904.2	-
7	86.02	583.8	16.52	4460.5	27.692	3008.6	4375.7
8	85.60	463.0	10.80	3831.1	27.785	2351.5	3763.3
9	85.60	169.9	10.66	2309.4	25.176	1607.7	-

Table A2. Oberhausen II operating parameters at NOMINAL LOAD (NL).

Operating Point	Mass Flow Rate (kg/s)	Temperature (°C)	Pressure (bar)	Specific Enthalpy (kJ/kg)	Specific Entropy (kJ/kg·K)	Specific Exergy (kJ/kg)	Isentropic Specific Enthalpy (kJ/kg)
1	91.69	24.3	10.79	1553.3	23.082	1476.0	-
2	89.46	83.8	15.83	1863.9	23.233	1741.5	1810.8
3	89.46	23.8	15.73	1552.3	22.290	1710.9	-
4	84.26	123.5	28.11	2073.9	22.589	2143.5	1958.8
5	84.26	435.5	27.43	3693.6	25.652	2849.8	-
6	84.26	743.6	25.92	5292.8	27.644	3855.1	-
7	89.74	568.3	15.20	4379.5	27.770	2904.3	4274.8
8	88.84	482.0	11.13	3930.2	27.855	2429.5	3866.4
9	88.84	179.5	11.02	2359.4	25.218	1645.0	-

Table A3. Oberhausen II operating parameters at 65% of NL.

Operating Point	Mass Flow Rate (kg/s)	Temperature (°C)	Pressure (bar)	Specific Enthalpy (kJ/kg)	Specific Entropy (kJ/kg·K)	Specific Exergy (kJ/kg)	Isentropic Specific Enthalpy (kJ/kg)
1	63.66	24.8	7.51	1554.9	23.843	1250.6	-
2	62.11	85.1	10.97	1869.1	24.013	1514.1	1809.2
3	62.11	24.3	10.95	1553.4	23.051	1485.2	-
4	58.50	124.1	19.57	2074.3	23.348	1917.6	1959.7
5	58.50	436.1	19.23	3694.3	26.394	2629.3	-
6	58.50	745.9	18.04	5302.5	28.409	3636.9	-
7	62.30	573.8	10.70	4406.9	28.533	2704.1	4303.2
8	61.48	488.8	7.80	3964.4	28.640	2229.9	3883.7
9	61.48	178.3	7.75	2352.1	25.935	1423.9	-

Table A4. Oberhausen II operating parameters at 45% of NL.

Operating Point	Mass Flow Rate (kg/s)	Temperature (°C)	Pressure (bar)	Specific Enthalpy (kJ/kg)	Specific Entropy (kJ/kg·K)	Specific Exergy (kJ/kg)	Isentropic Specific Enthalpy (kJ/kg)
1	44.73	24.0	5.15	1550.0	24.612	1016.3	-
2	43.64	85.7	7.58	1871.2	24.789	1284.7	1808.6
3	43.64	24.0	7.55	1550.7	23.818	1253.9	-
4	41.10	127.8	13.74	2091.6	24.130	1701.7	1970.2
5	41.10	432.5	13.46	3673.8	27.108	2395.9	-
6	41.10	742.8	12.68	5285.0	29.125	3405.8	-
7	43.69	564.9	7.45	4359.8	29.230	2449.3	4272.6
8	43.18	481.8	5.46	3927.5	29.333	1986.3	3850.5
9	43.18	175.5	5.31	2336.8	26.688	1184.1	-

References

1. Liu, Z.; Karimi, I.A. Gas turbine performance prediction via machine learning. *Energy* **2020**, *192*, 116627. [CrossRef]
2. Boyce, M.P. *Gas Turbine Engineering Handbook*; Elsevier: Amsterdam, The Netherlands, 2011.
3. Kotowicz, J.; Brzęczek, M. Analysis of increasing efficiency of modern combined cycle power plant: A case study. *Energy* **2018**, *153*, 90–99. [CrossRef]
4. Lorencin, I.; Anđelić, N.; Mrzljak, V.; Car, Z. Genetic algorithm approach to design of multi-layer perceptron for combined cycle power plant electrical power output estimation. *Energies* **2019**, *12*, 4352. [CrossRef]
5. Najjar, Y.S. Gas turbine cogeneration systems: A review of some novel cycles. *Appl. Therm. Eng.* **2000**, *20*, 179–197. [CrossRef]
6. Sun, L.; Wang, D.; Xie, Y. Energy, exergy and exergoeconomic analysis of two supercritical CO_2 cycles for waste heat recovery of gas turbine. *Appl. Therm. Eng.* **2021**, *196*, 117337. [CrossRef]
7. Rovira, A.; Sánchez, C.; Muñoz, M.; Valdés, M.; Durán, M.D. Thermoeconomic optimisation of heat recovery steam generators of combined cycle gas turbine power plants considering off-design operation. *Energy Convers. Manag.* **2011**, *52*, 1840–1849. [CrossRef]
8. Fernández, I.A.; Gómez, M.R.; Gómez, J.R.; Insua, Á.B. Review of propulsion systems on LNG carriers. *Renew. Sustain. Energy Rev.* **2017**, *67*, 1395–1411. [CrossRef]
9. Anđelić, N.; Šegota, S.B.; Lorencin, I.; Poljak, I.; Mrzljak, V.; Car, Z. Use of Genetic Programming for the Estimation of CODLAG Propulsion System Parameters. *J. Mar. Sci. Eng.* **2021**, *9*, 612. [CrossRef]
10. Mrzljak, V.; Mrakovčić, T. Comparison of COGES and diesel-electric ship propulsion systems. *Pomor. Zb.* **2016**, *1*, 131–148. [CrossRef]
11. Ekici, S.; Sohret, Y.; Coban, K.; Altuntas, O.; Karakoc, T.H. Performance evaluation of an experimental turbojet engine. *Int. J. Turbo Jet-Engines* **2017**, *34*, 365–375. [CrossRef]
12. Tuzcu, H.; Sohret, Y.; Caliskan, H. Energy, environment and enviroeconomic analyses and assessments of the turbofan engine used in aviation industry. *Environ. Prog. Sustain. Energy* **2021**, *40*, e13547. [CrossRef]
13. Aydin, H.; Turan, O.; Karakoc, T.H.; Midilli, A. Exergetic sustainability indicators as a tool in commercial aircraft: A case study for a turbofan engine. *Int. J. Green Energy* **2015**, *12*, 28–40. [CrossRef]
14. Balli, O. Exergy modeling for evaluating sustainability level of a high by-pass turbofan engine used on commercial aircrafts. *Appl. Therm. Eng.* **2017**, *123*, 138–155. [CrossRef]
15. Turan, Ö.; Aydın, H. Numerical calculation of energy and exergy flows of a turboshaft engine for power generation and helicopter applications. *Energy* **2016**, *115*, 914–923. [CrossRef]
16. Balli, O. Advanced exergy analyses of an aircraft turboprop engine (TPE). *Energy* **2017**, *124*, 599–612. [CrossRef]
17. Ibrahim, T.K.; Basrawi, F.; Awad, O.I.; Abdullah, A.N.; Najafi, G.; Mamat, R.; Hagos, F.Y. Thermal performance of gas turbine power plant based on exergy analysis. *Appl. Therm. Eng.* **2017**, *115*, 977–985. [CrossRef]
18. Saravanamuttoo, H.I.; Rogers, G.F.C.; Cohen, H. *Gas Turbine Theory*; Pearson Education: Hoboken, NJ, USA, 2001.
19. Kostyuk, A.; Frolov, V. *Steam and Gas Turbines*; Mir Publishers: Moscow, Russia, 1988.
20. Gouge, M.J. Closed cycle gas turbine nuclear power plant for submarine propulsion. *Nav. Eng. J.* **1995**, *107*, 35–41. [CrossRef]
21. Chen, L.G.; Zheng, J.L.; Sun, F.R.; Wu, C. Power, power density and efficiency optimization for a closed cycle helium turbine nuclear power plant. *Energy Convers. Manag.* **2003**, *44*, 2393–2401. [CrossRef]
22. Horlock, J.H. *Advanced Gas Turbine Cycles: A Brief Review of Power Generation Thermodynamics*; Elsevier: Amsterdam, The Netherlands, 2013.
23. Lee, J.C.; Campbell, J., Jr.; Wright, D.E. Closed-cycle gas turbine working fluids. *J. Eng. Power* **1981**, *103*, 220–228. [CrossRef]
24. Olumayegun, O.; Wang, M.; Kelsall, G. Closed-cycle gas turbine for power generation: A state-of-the-art review. *Fuel* **2016**, *180*, 694–717. [CrossRef]
25. McDonald, C.F. Helium turbomachinery operating experience from gas turbine power plants and test facilities. *Appl. Therm. Eng.* **2012**, *44*, 108–142. [CrossRef]
26. Kunniyoor, V.; Singh, P.; Nadella, K. Value of closed-cycle gas turbines with design assessment. *Appl. Energy* **2020**, *269*, 114950. [CrossRef]
27. Al-Attab, K.A.; Zainal, Z.A. Externally fired gas turbine technology: A review. *Appl. Energy* **2015**, *138*, 474–487. [CrossRef]
28. Hou, S.; Wu, Y.; Zhou, Y.; Yu, L. Performance analysis of the combined supercritical CO_2 recompression and regenerative cycle used in waste heat recovery of marine gas turbine. *Energy Convers. Manag.* **2017**, *151*, 73–85. [CrossRef]
29. Mrzljak, V.; Poljak, I.; Prpić-Oršić, J.; Jelić, M. Exergy analysis of marine waste heat recovery CO_2 closed-cycle gas turbine system. *Pomorstvo* **2020**, *34*, 309–322. [CrossRef]
30. Sharma, O.P.; Kaushik, S.C.; Manjunath, K. Thermodynamic analysis and optimization of a supercritical CO_2 regenerative recompression Brayton cycle coupled with a marine gas turbine for shipboard waste heat recovery. *Therm. Sci. Eng. Prog.* **2017**, *3*, 62–74. [CrossRef]
31. Hou, S.; Zhou, Y.; Yu, L.; Zhang, F.; Cao, S.; Wu, Y. Optimization of a novel cogeneration system including a gas turbine, a supercritical CO_2 recompression cycle, a steam power cycle and an organic Rankine cycle. *Energy Convers. Manag.* **2018**, *172*, 457–471. [CrossRef]
32. Hou, S.; Cao, S.; Yu, L.; Zhou, Y.; Wu, Y.; Zhang, F. Performance optimization of combined supercritical CO_2 recompression cycle and regenerative organic Rankine cycle using zeotropic mixture fluid. *Energy Convers. Manag.* **2018**, *166*, 187–200. [CrossRef]

33. Cao, Y.; Habibi, H.; Zoghi, M.; Raise, A. Waste heat recovery of a combined regenerative gas turbine-recompression supercritical CO_2 Brayton cycle driven by a hybrid solar-biomass heat source for multi-generation purpose: 4E analysis and parametric study. *Energy* **2021**, *236*, 121432. [CrossRef]
34. Kim, M.S.; Ahn, Y.; Kim, B.; Lee, J.I. Study on the supercritical CO_2 power cycles for landfill gas firing gas turbine bottoming cycle. *Energy* **2016**, *111*, 893–909. [CrossRef]
35. Invernizzi, C.M. Prospects of mixtures as working fluids in real-gas Brayton cycles. *Energies* **2017**, *10*, 1649. [CrossRef]
36. Keller, C. Forty years of experience on closed-cycle gas turbines. *Ann. Nucl. Energy* **1978**, *5*, 405–422. [CrossRef]
37. Bammert, K.; Krey, G.; Krapp, R. Operation and Control of the 50-MW Closed-Cycle Helium Turbine Oberhausen. In Proceedings of the Turbo Expo: Power for Land, Sea, and Air, American Society of Mechanical Engineers, Zurich, Switzerland, 30 March–4 April 1974. [CrossRef]
38. Bammert, K.; Deuster, G. Layout and present status of the closed-cycle helium turbine plant Oberhausen. In Proceedings of the Turbo Expo: Power for Land, Sea, and Air, American Society of Mechanical Engineers, Zurich, Switzerland, 30 March–4 April 1974. [CrossRef]
39. Bentivoglio, F.; Tauveron, N. Validation of the CATHARE2 code against Oberhausen II data. *Nucl. Technol.* **2008**, *164*, 55–75. [CrossRef]
40. Medica-Viola, V.; Šegota, S.B.; Mrzljak, V.; Štifanić, D. Comparison of conventional and heat balance based energy analyses of steam turbine. *Pomorstvo* **2020**, *34*, 74–85. [CrossRef]
41. Yazdi, M.R.M.; Ommi, F.; Ehyaei, M.A.; Rosen, M.A. Comparison of gas turbine inlet air cooling systems for several climates in Iran using energy, exergy, economic, and environmental (4E) analyses. *Energy Convers. Manag.* **2020**, *216*, 112944. [CrossRef]
42. Dincer, I.; Rosen, M.A. *Exergy: Energy, Environment and Sustainable Development*, 2nd ed.; Elsevier Science: Amsterdam, The Netherlands, 2012.
43. Mrzljak, V.; Lorencin, I.; Anđelić, N.; Car, Z. Thermodynamic Analysis of a Condensate Heating System from a Marine Steam Propulsion Plant with Steam Reheating. *J. Mar. Sci. Appl.* **2021**, *20*, 117–127. [CrossRef]
44. Koroglu, T.; Sogut, O.S. Conventional and advanced exergy analyses of a marine steam power plant. *Energy* **2018**, *163*, 392–403. [CrossRef]
45. Elhelw, M.; Al Dahma, K.S. Utilizing exergy analysis in studying the performance of steam power plant at two different operation mode. *Appl. Therm. Eng.* **2019**, *150*, 285–293. [CrossRef]
46. Kumar, A.K.B.A.; Nikam, K.C.; Behura, A.K. An exergy analysis of a 250 MW thermal power plant. *Renew. Energy Res. Appl.* **2020**, *1*, 197–204. [CrossRef]
47. Nedaei, N.; Hamrang, F.; Farshi, L.G. Design and 3E analysis of a hybrid power plant integrated with a single-effect absorption chiller driven by a heliostat field: A case study for Doha, Qatar. *Energy* **2022**, *239*, 122415. [CrossRef]
48. Fakhari, I.; Behinfar, P.; Raymand, F.; Azad, A.; Ahmadi, P.; Houshfar, E.; Ashjaee, M. 4E analysis and tri-objective optimization of a triple-pressure combined cycle power plant with combustion chamber steam injection to control NO_x emission. *J. Therm. Anal. Calorim.* **2021**, *145*, 1317–1333. [CrossRef]
49. Kabiri, S.; Khoshgoftar Manesh, M.H.; Amidpour, M. 4E analysis and evaluation of a steam power plant full repowering in various operations. *Energy Sources Part A Recovery Util. Environ. Eff.* **2020**, *42*, 1–21. [CrossRef]
50. Nikam, K.C.; Kumar, R.; Jilte, R. Economic and exergoeconomic investigation of 660 MW coal-fired power plant. *J. Therm. Anal. Calorim.* **2021**, *145*, 1121–1135. [CrossRef]
51. Rocha, D.H.; Silva, R.J. Exergoenvironmental analysis of a ultra-supercritical coal-fired power plant. *J. Clean. Prod.* **2019**, *231*, 671–682. [CrossRef]
52. Kanoğlu, M.; Çengel, Y.A.; Dincer, I. *Efficiency Evaluation of Energy Systems*; Springer Briefs in Energy: Berlin, Germany, 2012.
53. Aljundi, I.H. Energy and exergy analysis of a steam power plant in Jordan. *Appl. Therm. Eng.* **2009**, *29*, 324–328. [CrossRef]
54. Mrzljak, V.; Blecich, P.; Anđelić, N.; Lorencin, I. Energy and exergy analyses of forced draft fan for marine steam propulsion system during load change. *J. Mar. Sci. Eng.* **2019**, *7*, 381. [CrossRef]
55. Ahmadi, G.R.; Toghraie, D. Energy and exergy analysis of Montazeri steam power plant in Iran. *Renew. Sustain. Energy Rev.* **2016**, *56*, 454–463. [CrossRef]
56. Mrzljak, V.; Poljak, I.; Medica-Viola, V. Dual fuel consumption and efficiency of marine steam generators for the propulsion of LNG carrier. *Appl. Therm. Eng.* **2017**, *119*, 331–346. [CrossRef]
57. Tan, H.; Shan, S.; Nie, Y.; Zhao, Q. A new boil-off gas re-liquefaction system for LNG carriers based on dual mixed refrigerant cycle. *Cryogenics* **2018**, *92*, 84–92. [CrossRef]
58. Kaushik, S.C.; Reddy, V.S.; Tyagi, S.K. Energy and exergy analyses of thermal power plants: A review. *Renew. Sustain. Energy Rev.* **2011**, *15*, 1857–1872. [CrossRef]
59. Erdem, H.H.; Akkaya, A.V.; Cetin, B.; Dagdas, A.; Sevilgen, S.H.; Sahin, B.; Teke, I.; Gungor, C.; Atas, S. Comparative energetic and exergetic performance analyses for coal-fired thermal power plants in Turkey. *Int. J. Therm. Sci.* **2009**, *48*, 2179–2186. [CrossRef]
60. Noroozian, A.; Mohammadi, A.; Bidi, M.; Ahmadi, M.H. Energy, exergy and economic analyses of a novel system to recover waste heat and water in steam power plants. *Energy Convers. Manag.* **2017**, *144*, 351–360. [CrossRef]
61. Adibhatla, S.; Kaushik, S.C. Energy and exergy analysis of a super critical thermal power plant at various load conditions under constant and pure sliding pressure operation. *Appl. Therm. Eng.* **2014**, *73*, 51–65. [CrossRef]
62. Szargut, J. *Exergy Method: Technical and Ecological Applications*; WIT Press: Southampton, UK, 2005.

63. Lemmon, E.W.; Huber, M.L.; McLinden, M.O. *NIST Standard Reference Database 23, Reference Fluid Thermodynamic and Transport Properties (REFPROP)*, version 9.0; National Institute of Standards and Technology: Gaithersburg, MD, USA, 2010.
64. Mrzljak, V.; Poljak, I.; Mrakovčić, T. Energy and exergy analysis of the turbo-generators and steam turbine for the main feed water pump drive on LNG carrier. *Energy Convers. Manag.* **2017**, *140*, 307–323. [CrossRef]
65. Kopac, M.; Hilalci, A. Effect of ambient temperature on the efficiency of the regenerative and reheat Çatalağzı power plant in Turkey. *Appl. Therm. Eng.* **2007**, *27*, 1377–1385. [CrossRef]
66. Wartsila-Combustion Engine vs. Gas Turbine: Part Load Efficiency and Flexibility. Available online: https://www.wartsila.com/energy/learn-more/technology-comparison-engine-vs-aero/combustion-engine-vs-gas-turbine-part-load-efficiency-and-flexibility (accessed on 15 May 2023).
67. Najjar, Y.S.; Alalul, O.F.; Abu-Shamleh, A. Degradation analysis of a heavy-duty gas turbine engine under full and part load conditions. *Int. J. Energy Res.* **2020**, *44*, 4529–4542. [CrossRef]
68. Najjar, Y.S.; Alalul, O.F.; Abu-Shamleh, A. Steam turbine bottoming cycle deterioration under different load conditions. *Therm. Sci. Eng. Prog.* **2020**, *20*, 100733. [CrossRef]
69. Nirbito, W.; Budiyanto, M.A.; Muliadi, R. Performance Analysis of Combined Cycle with Air Breathing Derivative Gas Turbine, Heat Recovery Steam Generator, and Steam Turbine as LNG Tanker Main Engine Propulsion System. *J. Mar. Sci. Eng.* **2020**, *8*, 726. [CrossRef]